



Published in final edited form as:

Nature. 2018 May ; 557(7706): 570–574. doi:10.1038/s41586-018-0121-3.

Mxra8 is a receptor for multiple arthritogenic alphaviruses

Rong Zhang¹, Arthur S. Kim^{1,5}, Julie M. Fox¹, Sharmila Nair¹, Katherine Basore⁵, William B. Klimstra², Rebecca Rimkunas⁴, Rachel H. Fong⁴, Hueylie Lin¹, Subhajit Poddar¹, James E. Crowe Jr.³, Benjamin J. Doranz⁴, Daved H. Fremont⁵, and Michael S. Diamond^{1,5,6,7,*}

¹Department of Medicine, Washington University School of Medicine, Saint Louis, MO 63110 USA

²University of Pittsburgh Center for Vaccine Research, Pittsburgh, PA 15261 USA

³Vanderbilt Vaccine Center, Department of Pediatrics, and Department of Pathology, Microbiology and Immunology, Vanderbilt University Medical Center, Nashville, TN 37232 USA

⁴Integral Molecular, Inc., Philadelphia, PA, 19104 USA

⁵Department of Pathology and Immunology, Washington University School of Medicine, Saint Louis, MO 63110 USA

⁶Department of Molecular Microbiology, Washington University School of Medicine, Saint Louis, MO 63110 USA

⁷Andrew M. and Jane M. Bursky The Center for Human Immunology and Immunotherapy Programs, Washington University School of Medicine, Saint Louis, MO 63110 USA

Abstract

Arthritogenic alphaviruses comprise a group of enveloped RNA viruses that are transmitted to humans by mosquitoes and cause debilitating acute and chronic musculoskeletal disease¹. The host factors required for alphavirus entry remain poorly characterized². Using a genome-wide CRISPR/Cas9-based screen, we identified the cell adhesion molecule Mxra8 as an entry mediator for multiple emerging arthritogenic alphaviruses including chikungunya (CHIKV), Ross River, Mayaro, and O'nyong nyong (ONNV) viruses. Gene editing of mouse *Mxra8* or human *MXRA8* resulted in reduced viral infection of cells, and reciprocally, ectopic expression resulted in increased infection. Mxra8 bound directly to CHIKV particles and enhanced virus attachment and

Users may view, print, copy, and download text and data-mine the content in such documents, for the purposes of academic research, subject always to the full Conditions of use: http://www.nature.com/authors/editorial_policies/license.html#terms Reprints and permissions information is available at www.nature.com/reprints.

*Address correspondence to: Michael S. Diamond, M.D. Ph.D., Departments of Medicine, Molecular Microbiology, and Pathology and Immunology, Washington University School of Medicine, 660 South Euclid Ave. Box 8051, Saint Louis, MO 63110, USA. diamond@borcim.wustl.edu, (314) 362-2842.

Correspondence. Address requests for materials to diamond@wusm.wustl.edu.

M.S.D. is a consultant for Inbios and Sanofi-Pasteur and on the Scientific Advisory Board of Moderna. J.E.C. is on the Scientific Advisory Boards of GigaGen, Meissa Vaccines, and PaxVax, and is a Founder of IDBiologics. B.J.D. is a shareholder of Integral Molecular.

AUTHOR CONTRIBUTIONS

R.Z. performed CRISPR-Cas9 screening and infection studies with J.M.F., S.N., H.L., and S.P. A.S.K. generated Mxra8-Fc and performed ELISAs. K.B. performed SPR experiments. R.R. and R.H.F. performed mapping experiments. R.Z., A.S.K., J.M.F., B.J.D., D.H.F., and M.S.D. designed experiments. W.B.K. and J.E.C. provided key reagents. R.Z., A.S.K., J.M.F., K.B., R.H.F., and B.J.D. performed data analysis. R.Z. and M.S.D. wrote the initial manuscript draft.

internalization into cells. Consistent with these findings, Mxra8-Fc protein or anti-Mxra8 monoclonal antibodies blocked CHIKV infection in multiple cell types including primary human synovial fibroblasts, osteoblasts, chondrocytes, and skeletal muscle cells. Mutagenesis experiments suggest that Mxra8 binds to a surface-exposed region across the A and B domains of CHIKV E2, a speculated site of attachment. Finally, administration of Mxra8-Fc protein or anti-Mxra8 blocking antibodies reduced CHIKV or ONNV infection and associated foot swelling in mice. Pharmacological targeting of Mxra8 could form a strategy for mitigating infection and disease by multiple arthritogenic alphaviruses.

We performed a genome-wide screen for host factors required for chikungunya virus (CHIKV) infection using the CRISPR/Cas9 system^{3,4} and lentiviruses delivering single-guide RNA (sgRNA) targeting 20,611 mouse genes (Extended Data Fig 1a). We inoculated lentivirus-transduced 3T3 mouse fibroblasts with CHIKV-181/25-mKate2, such that virtually all cells expressed the reporter gene by 24 h. The few cells lacking mKate2 expression were sorted, propagated in the presence of neutralizing anti-CHIKV mAbs⁵, and then re-inoculated with CHIKV-181/25-mKate2. After two rounds of infection and sorting, genomic DNA from mKate2-negative cells was harvested, sgRNAs were sequenced, and analyzed using MAGeCK⁶ (Supplementary Tables 1 and 2). The top candidate was *Mxra8* (also called DICAM, ASP3, or limitrin), an adhesion molecule found in mammals, birds, and amphibians (Extended Data Fig 1b–c), that is expressed on epithelial, myeloid, and mesenchymal cells^{7–10} and shares homology with junctional adhesion molecule⁹, a reovirus entry receptor¹¹. We validated *Mxra8* using three different sgRNAs in bulk 3T3 cells, by generating Δ *Mxra8* single-cell clones in 3T3 and MEF cells, and confirming gene deletion and cell viability (Extended Data Fig 2a–e). Infection of CHIKV-181/25 was reduced in Δ *Mxra8* cells, and trans-complementation of *Mxra8* in Δ *Mxra8* 3T3 cells restored infectivity (Fig 1a–b). As CHIKV-181/25 is a cell culture-adapted vaccine strain¹² that has acquired heparan sulfate (HS) binding activity¹³, we evaluated Mxra8 with other CHIKV strains. Infection of CHIKV-AF15561, the parental Asian strain of CHIKV-181/25, which binds poorly to HS¹⁴, and CHIKV-37997, a West African strain, was abolished in Δ *Mxra8* 3T3 cells, reduced in Δ *Mxra8* MEFs (Fig 1a), and restored in trans-complemented Δ *Mxra8* 3T3 cells (Fig 1b–c). However, the dependence on Mxra8 was less with CHIKV-LR 2006, an East Central South African strain (Fig 1a and d). To confirm that CHIKV required Mxra8 independently of HS binding, we expressed murine Mxra8 in parental or glycosaminoglycan-deficient Chinese hamster ovary (CHO) cells¹⁵ (Extended Data Fig 3a). Expression of Mxra8 enhanced infectivity of CHIKV regardless of whether CHO cells expressed HS or other glycosaminoglycans (Extended Data Fig 3b–c).

We tested the requirement of Mxra8 for infection by other alphaviruses. Whereas Mayaro, Ross River, ONNV, and Barmah Forest arthritogenic alphaviruses showed reduced infection in Δ *Mxra8* 3T3 cells, Semliki Forest and Getah viruses had partial phenotypes, and other related alphaviruses (Sindbis [SINV], Bebaru, Una, and Middleburg) showed little dependence on Mxra8 (Fig 1e and Extended Data Fig 4). Minimal differences in infection were observed between control and Δ *Mxra8* 3T3 cells with chimeric SINV expressing the structural genes of the encephalitic Eastern (EEEV) or Western (WEEV) equine encephalitis alphaviruses or a Venezuelan equine encephalitis virus (VEEV-GFP) (Fig 1e). No effect of

Mxra8 was seen on infection of unrelated positive- or negative-sense RNA viruses (Fig 1f). We next assessed whether any of the four isoforms of the human *MXRA8* ortholog (Extended Data Fig 1b) served a similar function. As HeLa cells did not express *MXRA8* (Extended Data Fig 5), we used these cells for ectopic expression (Extended Data Fig 6a). *MXRA8*-1, -2, and -4 but not *MXRA8*-3 were detected on the cell surface, and *MXRA8*-1 and -2 enhanced CHIKV infectivity (Fig 1g). Similarly, expression of *MXRA8*-2 in A549 or 293T cells resulted in greater CHIKV infection (Extended Data Fig 6b–c). Consistent with this observation, expression of different sgRNAs targeting all isoforms of *MXRA8* in MRC-5 human lung fibroblasts (MRC-5), foreskin fibroblasts (HFF-1), retinal pigment epithelial cells (RPE), and fibrosarcoma cells (Hs 633T) resulted in less CHIKV infection than in control gene-edited cells (Fig 1h and Extended Data Fig 7a–b).

To determine whether *Mxra8* is required for replication, we transfected CHIKV genomic RNA into control and Δ *Mxra8* MEFs in the presence of NH_4Cl to inhibit virus maturation and further rounds of infection. As no difference in CHIKV gene expression was detected (Fig 2a), *Mxra8* does not appear to affect translation or replication. We demonstrated a *Mxra8*-dependence of the structural proteins using pseudotyped viruses. Whereas infection of CHIKV pseudotyped virions encapsidating a murine leukemia virus GFP-reporter RNA was reduced in Δ *Mxra8* compared to control MEFs, infection of EEEV or WEEV pseudotyped virions was not (Fig 2b). Consistent with a role for *Mxra8* in the entry pathway, CHIKV-AF15561 showed reduced binding at 4°C to Δ *Mxra8* compared to control MEFs, and increased binding to cells over-expressing *Mxra8* (Fig 2c–d). When virus internalization assays were performed at 37°C, less CHIKV RNA was measured within Δ *Mxra8* MEFs, and more CHIKV RNA was detected in cells over-expressing *Mxra8* (Fig 2c).

To corroborate an effect of *Mxra8* on binding and entry, we generated Fc fusion proteins with the extracellular domains of mouse *Mxra8* or human *MXRA8*-2 along with a control (osteoprotegerin [OPG]) protein (Extended Data Fig 8a). Pre-incubation with *Mxra8*-Fc or *MXRA8*-2-Fc, but not the control OPG-Fc reduced CHIKV-181/25 infection in 3T3 (Fig 2e) or MRC-5 (Fig 2f) cells. We tested a panel of seven, hamster monoclonal antibodies (mAbs) against mouse *Mxra8* (Extended Data Fig 8b) for their capacity to inhibit CHIKV infection. All seven mAbs bound to mouse *Mxra8*-Fc, with four also recognizing human *MXRA8*-2-Fc (Extended Data Fig 8c). Pre-treatment of 3T3 cells with anti-*Mxra8* mAbs reduced CHIKV infection (Fig 2g). Three of the mAbs that bound human *MXRA8*-2-Fc also reduced infection in MRC-5 cells (Extended Data Fig 8d). To establish the importance of the *Mxra8* ectodomain, we engineered forms with glycosphosphatidylinositol (GPI) anchors or lacking a cytoplasmic domain (Δ C-tail) for trans-complementation (Extended Data Fig 9). Notably, *Mxra8*-GPI and *Mxra8*- Δ C-tail restored CHIKV infection (Fig 2h). Interaction with the *Mxra8* ectodomain may facilitate viral glycoprotein conformational changes that are required for internalization or fusion¹⁶ or potentiate interactions with other host factors that bridge membrane penetration and entry¹⁷. Finally, heterologous expression of human *MXRA8*-2 in Δ *Mxra8* mouse cells also restored CHIKV infection (Fig 2h).

To determine whether *Mxra8* directly binds to CHIKV, we captured virions or virus-like particles (VLPs)¹⁸ with a human anti-CHIKV mAb¹⁹, and added *Mxra8*-Fc or *MXRA8*-2-Fc in an ELISA. Both *Mxra8*-Fc and *MXRA8*-2-Fc but not OPG-Fc bound to CHIKV

virions and VLPs (Fig 3a–b). In comparison, Mxra8-Fc and MXRA8-2-Fc did not bind efficiently to SINV-EEEV (Fig 3c). In a complementary assay, we assessed binding of Mxra8-Fc protein to cell-surface displayed alphavirus proteins on infected cells^{19,20}. Mxra8-Fc bound CHIKV, ONNV, MAYV, RRV-infected cells, but not SINV or VEEV-infected cells (Extended Data Fig 10a–b). We also analyzed binding of Mxra8 to CHIKV VLPs by surface plasmon resonance, and found a slow association rate, a long half-life, and an affinity of ~200 nM (Fig 3d).

We evaluated whether human anti-CHIKV mAbs that bound epitopes within the E2 protein¹⁹ altered Mxra8-Fc binding to CHIKV. Several mAbs recognizing epitopes in the A domain (2H1, 8G18, 3E23, and 1O6) or shared epitopes in the A and B domains (1H12 and 4J14) inhibited binding, whereas others localizing to distinct sites had less effect (Fig 3e). We then tested binding of Mxra8-Fc to an alanine scanning mutagenesis library of E2 A and B domains in the context of display on the surface of 293T cells^{19,20}. Residues W64, D71, T116, and I121 in the A domain and I190, Y199, and I217 in the B domain of E2 emerged as essential for optimal Mxra8-Fc binding (Fig 3f and Supplementary Table 3) and overlap the binding sites of the blocking mAbs tested¹⁹. Mapping of these residues onto the pE2-E1 heterodimer or the trimer of heterodimers (Extended Data Fig 10c–d) on the virion surface²¹ revealed a solvent-accessible epitope across the top of the A and B domains, a proposed site of alphavirus receptor engagement^{22,23}.

To begin to assess the physiological importance of MXRA8 interaction with CHIKV, we tested surface expression of MXRA8 on primary human keratinocytes (KE), dermal fibroblasts (DF), synovial fibroblasts (SF), osteoblasts (OB), chondrocytes (CH), and skeletal muscle cells (SMC) (Fig 4a), which are targets of infection by alphaviruses²⁴. Pretreatment with anti-MXRA8 blocking mAbs inhibited infection of CHIKV-AF15561 in all cells but keratinocytes, which lack MXRA8 expression (Fig 4a–b). We next evaluated whether co-injection of Mxra8-Fc with CHIKV-AF15561 would diminish infection in C57BL/6 mice. Addition of Mxra8-Fc diminished CHIKV infection in the ipsilateral ankle and muscle (Fig 4c) and reduced foot swelling (Fig 4d) compared to a control mAb. Treatment with Mxra8-Fc also inhibited ONNV infection in the ipsilateral ankle of mice (Fig 4e). We next administered Mxra8-Fc via an intraperitoneal route and 6 h later inoculated CHIKV in the footpad. Mxra8-Fc treatment reduced foot swelling and viral burden in the ipsilateral ankle (Fig 4f–g), although the phenotype was less than in co-injection experiments. To extend these findings, we transferred hamster anti-Mxra8 blocking or control mAbs to mice via an intraperitoneal route 12 h prior to CHIKV inoculation. Reduced CHIKV titers were observed in the ipsilateral ankle and calf muscle, and contralateral ankle at 12 and 72 h after infection in anti-Mxra8 compared to control mAb-treated mice (Fig 4h). Treatment with anti-Mxra8 mAbs also reduced foot swelling (Fig 4i). In post-exposure therapeutic experiments, we observed reduced CHIKV infection in the contralateral ankle and muscle when anti-Mxra8 mAbs was administered at 8 or 24 h after virus inoculation (Fig 4j and Extended Data Fig 8e). These *in vivo* experiments establish a function for Mxra8 in the pathogenesis of infection of arthritogenic alphaviruses.

Our studies establish that mouse Mxra8 contributes to CHIKV entry and is required for infection and disease. Human MXRA8 also bound CHIKV and supported infection, and

MXRA8 expression in primary human cells overlapped with the tropism of CHIKV *in vivo*. Remarkably, infection of several arthritogenic alphaviruses (*e.g.*, CHIKV, ONNV, MAYV, and RRV) was reduced in $\Delta Mxra8$ cells, suggesting Mxra8 may serve as a shared receptor. These data contrast with natural resistance-associated macrophage protein (NRAMP2), which is an entry receptor for SINV but not for CHIKV or RRV²⁵. Nonetheless, residual CHIKV infection in the absence of Mxra8 in cells and *in vivo* and the absence of an apparent mosquito ortholog suggest that additional unidentified host factors contribute to cell binding and entry.

Our mutagenesis mapping studies suggest that amino acids in the E2 A and B domains contribute to the interaction of CHIKV with Mxra8. Higher resolution structural experiments are needed to define the complete footprint of binding between Mxra8 and CHIKV E2 protein. Such studies could facilitate the development of small molecules or biologicals that disrupt Mxra8 interaction with E2 protein, which could form the basis of therapeutics that ameliorate disease caused by multiple emerging alphaviruses.

METHODS

Cells and viruses

Vero, NIH-3T3, MEFs, HEK 293T, A549, HeLa (ATCC #CCL-2), MRC-5 (provided by D. Wang, Washington University), HFF-1 (ATCC #SCRC-1041), Hs 633T (Sigma-Aldrich #89050201), Huh7, RPE (provided by M. Mahjoub, Washington University), JEG3, U2OS (provided by S. Cherry, University Of Pennsylvania), HT1080 (provided by J. Cooper, Washington University), Raji, and K562 cells all were cultured at 37°C in Dulbecco's Modified Eagle Medium supplemented with 10% fetal bovine serum (FBS), 10 mM HEPES, 1 mM Sodium pyruvate, 1× non-essential amino acids, and 100 U/mL of Penicillin-Streptomycin. HTR8/SV.neo cells were cultured in RPMI 1640 supplemented with 5% FBS and 1% penicillin and streptomycin. Jurkat cells were cultured at 37°C in RPMI 1640 supplemented with 10% FBS and 10 mM HEPES. hCMEC/D3 cells (provided by R. Klein, Washington University) were cultured in EBM-2 media (Lonza, 00190860) supplemented with 5% FBS, 5 µg/mL ascorbic acid, 10 mM HEPES, 1% Lipid concentrate (Gibco, 11905-031) in plates pre-coated with collagen. All cell lines were tested and judged free of mycoplasma contamination using a commercial kit.

Primary human keratinocytes (#102-05n), synovial fibroblasts (#408-05a), osteoblasts (#406-05f), chondrocytes (#402-05f), and skeletal muscle cells (#S150-05f) were purchased from Cell Applications. Primary human dermal fibroblasts (#CC-2509) were obtained from Lonza. Cells were thawed and cultured in specified medium according to the instructions of the manufacturers, and used within one week.

The following alphaviruses were used: CHIKV (strains 2006 La Reunion OPY1, 37997, AF15561, 181/25, and 181/25-mKate2 (rescued from pJM6 CHIKV-181/25 mKate2 cDNA clone, provided by T. Morrison and M. Heise), RRV (T48), MAYV (BeH407), ONNV (MP30), Semliki Forest (Kumba), SINV (Toto1101, Girdwood), Bebaru (MM 2354), Middleburg (30037), Getah (AMM-2021), Una (CoAr2380), and Barmah Forest (K10521) viruses. Additional viruses tested included chimeric encephalitic alphaviruses (SINV-EEEV,

SINV-WEEV, and VEEV-GFP (TC-83)), a flavivirus (WNV, New York 2000), a bunyavirus (RVFV-GFP, MP-12), a rhabdovirus (VSV-GFP, Indiana), and a picornavirus (encephalomyocarditis virus, EMCV). Replication-competent SINV chimeric viruses were constructed by replacing the SINV TR339 structural protein genes with EEEV FL93-939 or WEEV Fleming structural protein genes under control of the SINV subgenomic promoter in the TR339 cDNA clone²⁶. All viruses were propagated in Vero cells and titrated by standard plaque or focus-forming assays²⁷.

Pooled sgRNA screen and data analysis

A mouse GeCKOv2 CRISPR knockout pooled library encompassing 130,209 different sgRNAs against 20,611 genes²⁸ was made available by Feng Zhang (Addgene #100000053), and amplified in Endura cells (Lucigen # 60242) as described previously^{28,29}. The sgRNA library was divided in half (A + B), packaged into lentiviruses, and used for independent screening. The sgRNA plasmid library was packaged in 293FT cells after co-transfection with psPAX2 (Addgene #12260) and pMD2.G (Addgene #12259) at a ratio of 2:2:1 using Fugene®HD (Promega). Approximately 48 h after transfection, supernatants were harvested, clarified by centrifugation (3,500 rpm x 20 min) and aliquotted for storage at -80°C.

For the CRISPR screen, a clonal 3T3-Cas9 cell line was generated by transduction with a packaged lentivirus (lentiCas9-Blast, Addgene #52962), blasticidin selection, and limiting dilution. 3T3-Cas9 cells were expanded and transduced with CRISPR sgRNA lentivirus library at a multiplicity of infection (MOI) of 0.3 by spinoculation (1,000 x g) at 32°C for 30 min in 12-well plates. After selection with puromycin for 7 days, $\sim 1 \times 10^8$ cells were inoculated with CHIKV-181/25-mKate2 (MOI of 1) and then incubated for 24 h to allow nearly all cells to become infected. Cells were sorted for an absence of mKate2 expression using a Sony Biotechnology Synergy SY3200 Cell sorter (Siteman Flow Cytometry Core, Washington University). To enrich for the cell population that was resistant to CHIKV infection and increase the signal-to-noise ratio, the mKate2-negative cells were expanded in culture. Given the rapid replication rate and cytopathic effect of CHIKV, two humanized neutralizing mAbs⁵, CHK-152 and CHK-166 (2 µg/ml of each), were added to block infection by any residual virus. The expanded cells were re-infected with CHIKV-181/25-mKate2 in the absence of mAbs, sorted for mKate2 negative cells, and the procedure was repeated for one additional round.

Genomic DNA was extracted from the uninfected cells (5×10^7) or the mKate2-negative sorted cells (1×10^7), and sgRNA sequences were amplified³⁰, and subjected to next generation sequencing using an Illumina HiSeq 2500 platform (Genome Technology Access Center, Washington University). The sgRNA sequences against specific genes were determined after removal of the tag sequences using the FASTX-Toolkit (http://hannonlab.cshl.edu/fastx_toolkit/) and cutadapt 1.8.1. sgRNA sequences were analyzed using a published computational tool (MAGECK)⁶ (see Supplementary Tables 1 and 2).

Gene validation

Mxra8 was validated by using three independent sgRNAs as follows: *Mxra8*-sgRNA1, 5'-CTTGTGGATATGTATTCGGC-3'; *Mxra8*-sgRNA2, 5'-TGTGCGCCTCGAGGTTACAG-3'; *Mxra8*-sgRNA3, 5'-GCTGCATGATCGCCAGCGCG-3'. The sgRNAs were cloned into the plasmid lentiCRISPR v2 (Addgene #52961) and packaged with lentivirus express system. 3T3 or MEFs cells were transduced with lentiviruses expressing individual sgRNA and selected with puromycin for 7 days prior to infection with different viruses. For some validation experiments, clonal cells edited by sgRNA1 were isolated by limiting dilution. To validate the human ortholog *MXRA8*, two different sgRNAs targeting all four isoforms were used: *MXRA8*-sgRNA1, 5'-GGCGCGGATGCCTTTGAGCG-3'; *MXRA8*-sgRNA2, 5'-GTCCGCCTGGAGGTCACCGA-3'. The sgRNAs were cloned similarly as above, and the gene-edited bulk cells were used for validation studies.

For flow cytometric analyses, gene-edited 3T3 cells were inoculated with different viruses as follows: CHIKV-181/25 (MOI of 3, 9.5 h), CHIKV-AF15561 (MOI of 10, 24 h), CHIKV-37997 (MOI of 3, 10 h), CHIKV-LR 2006 (MOI of 1, 9.5 h), ONNV (MOI of 3, 12 h), RRV (MOI of 3, 32 h), MAYV (MOI of 3, 24 h), SFV (MOI of 1, 9 h), SINV (MOI of 10, 6 h), SIN-WEEV (MOI of 10, 10 h), SIN-EEEV (MOI of 10, 10 h), VEEV-GFP (MOI of 3, 6.5 h), RVFV-GFP (MOI of 10, 8 h), VSV-GFP (MOI of 3, 6 h), WNV (MOI of 10, 25 h), and EMCV (MOI of 3, 6 h). Gene-edited MEF cells were inoculated with CHIKV-181/25 (MOI of 3, 8 h), CHIKV-AF15561 (MOI of 10, 10h), CHIKV-37997 (MOI of 1, 10 h), and CHIKV-LR 2006 (MOI of 1, 8 h). Gene-edited MRC-5, RPE, and HFF-1 cells were inoculated with CHIKV-181/25 (MOI of 10, 10 h), CHIKV-AF15561 (MOI of 10, 10 h), and CHIKV-LR 2006 (MOI of 1, 10 h). Gene-edited Hs 633T cells were inoculated with CHIKV-181/25 (MOI of 15), CHIKV-AF15561 (MOI of 15), and CHIKV-LR 2006 (MOI of 3) for 11.5 h. At the indicated times, cells were harvested with trypsin, and fixed with 1% paraformaldehyde (PFA) diluted in PBS for 15 min at room temperature and permeabilized with Perm buffer (HBSS supplemented with 10 mM HEPES, 0.1% (w/v) saponin, and 2% FBS) for 10 min at room temperature. Cells then were incubated for 30 min at room temperature with 1 µg/ml of the following virus-specific antibodies: CHIKV (mouse CHK-11⁵), ONNV and MAYV (mouse CHK-48), RRV (human 1I9); SINV (ascites fluid, ATCC VR-1248AF), SFV (mouse CHK-124), VEEV (mouse 1A4A), WEEV (mouse 11A1), EEEV (mouse EEEV-10), WNV (human E16³¹), EMCV (mouse serum). After washing, cells were incubated with 2 µg/ml of Alexa Fluor 647-conjugated goat anti-mouse or anti-human IgG (Invitrogen) for 30 min at room temperature. Cells were processed on a MACSQuant® Analyzer 10 (Miltenyi Biotec), and analyzed using FlowJo software (Tree Star).

Validation also was performed by an infectious virus yield assay. Gene-edited 3T3 cells were plated 12 h prior to infection. Cells were inoculated with CHIKV-181/25, CHIKV AF15561, CHIKV-LR 2006 at an MOI of 0.01 or other alphaviruses (BEBV, MOI 0.001; BFV, GETV, UNAV, MIDV, and SFV, all at MOI of 0.01) for 1 h, then washed once and maintained in reduced 2% FBS culture media. Supernatants were harvested at specific times after infection

for titration on Vero cells by focus-forming assay (CHIKV) or standard plaque assay (all other viruses).

Genomic RNA transfection and analysis

To assess for effects of Mxra8 on CHIKV replication, we transfected capped viral genomic RNA into MEFs. Capped genomic RNA was generated using an mMESSAGE mMACHINE™ SP6 Transcription Kit according to the manufacturer's instructions (Thermo Fisher Scientific #AM1340) from the *NotI*-linearized CHIKV-181/25 cDNA clone. 1 µg of purified RNA was transfected into control or Δ Mxra8 cells using the Neon transfection system according to the manufacturer's instructions (Thermo Fisher Scientific). Cells were then incubated in 15 mM NH₄Cl to prevent subsequent rounds of infection. At specified times, cells were harvested with trypsin and processed for E2 expression levels by flow cytometry.

Pseudotyped virus experiments

MLV-GFP pseudoviruses were made as described^{32,33} except plasmids encoding structure proteins of CHIKV (strain 37997), VEEV (strain TrD), and EEEV (strain FL91-4697) were used. Pseudovirus entry in 3T3 cells expressing or lacking Mxra8 was assessed 36 h later by measuring GFP expression by flow cytometry.

Plasmid construction

The C-terminal FLAG tagged mouse Mxra8 corresponding to the transcript (NM_024263) was synthesized (Integrated DNA Technologies, Inc.) and cloned into the lentivirus vector pCSII-EF1-IRES-Venus with restriction sites *NotI*/*Bam*HI. The Mxra8 sgRNA target sequences were mutated (ctgtggatgtattcggcg to ctGgtCgaCatgtaCAGCgcg) to avoid re-cutting by Cas9 protein for the trans-complementation assay. Based on this plasmid, a truncation lacking the cytoplasmic domain was constructed by PCR-mediated mutagenesis Δ C-tail (378-442). To express the GPI anchored Mxra8, the N-terminal 336 amino acids missing the transmembrane and cytoplasmic domains were fused with placental alkaline phosphatase (PLAP)
(ctggcgccecccccgcggcaccaccgacccgcgcgcccggggcggtccgtggtccccgcgttcttctctgctgcccgggac cctgctgctgctggagacggcactgctccc) or Qa1
(taccatacagatgtccagattacgctacgtctcaccatccattggcgcccaaatgactttactattggccatgatcatgtttgcgt taaagatagggtcg, HA tag is underlined) GPI anchor sequences. To assess the function of different human MXRA8 isoforms, the cDNA of isoform 2 (NM_032348.3) containing C-terminal Myc and FLAG tags was purchased from OriGene (Cat. No. RC200955), and cloned into the lentivirus vector pCSII-EF1-IRES-Venus. The Isoform 1 (NM_001282585.1), isoform 3 (NM_001282584.1), and isoform 4 (NM_001282583.1) were created by either mutagenesis of isoform 2 or gene synthesis (Integrated DNA Technologies, Inc.), and cloned into the lentivirus vector pCSII-EF1-IRES-Venus containing C-terminus Myc and FLAG tags.

Trans-complementation and ectopic expression experiments

The plasmids constructed above were packaged using the lentivirus expression system. Cells transduced with these lentiviruses were sorted for Venus-positive cells by flow cytometry. 3T3 cells were inoculated with CHIKV-181/25 (MOI 3) for 9.5 h, or CHIKV-AF15561 (MOI 10) for 20 h. HeLa and A549 cells were inoculated with CHIKV-181/25 (MOI 3), CHIKV-AF15561 (MOI 10), or CHIKV-LR 2006 (MOI 1) for 14 h. 293T cells were inoculated with CHIKV-181/25 (MOI 1), CHIKV-AF15561 (MOI 3), or CHIKV-LR 2006 (MOI 0.5) for 11.5 h. CHO cells (K1 and 745) were inoculated with CHIKV-181/25 (MOI 0.3), CHIKV-AF15561 (MOI 10), or CHIKV-LR 2006 (MOI 0.3) for 12 h. Cells were then harvested and processed for E2 expression by flow cytometry.

Generation and production of Mxra8-Fc and MXRA8-2-Fc

A cDNA fragment encoding the mouse Mxra8 extracellular domain (residues 22-336, GenBank accession no. NM_024263) or the human MXRA8-2 extracellular domain (residues 20-337, GenBank accession no. NM_032348.3) and the mouse IgG2a-Fc were synthesized (Integrated DNA Technologies) and inserted into the pCDNA3.4 vector (Thermo Fisher) downstream of an IL-22 signal peptide sequence. After confirmation by Sanger sequencing, Mxra8-Fc and MXRA8-2-Fc were expressed into Expi293 cells (Thermo Fisher). Cells were seeded at 5×10^6 cells/ml one day prior to transfection. 200 μ g of plasmid was diluted in Opti-MEM (Thermo Fisher) and complexed with HYPE-5 transfection reagent before addition to cells. Transfected cells were supplemented daily with Expi293 media and 2% (w/v) Hyclone Cell Boost. Four days after transfection, supernatant was harvested, centrifuged at $3,000 \times g$ for 15 min, and purified by Protein A Sepharose 4B (Thermo Fisher) chromatography. After elution and buffer neutralization, the purified protein was dialyzed into 20 mM HEPES, 150 mM NaCl (pH 7.5), filtered through a 0.2 μ m filter, and stored at -80°C . Mxra8 that was cleaved from the IgG backbone was generated by inserting an HRV cleavage sequence (LEVLFGQP) into Mxra8-Fc downstream of the Mxra8 coding sequence and prior to the mouse IgG sequence. Mxra8-HRV-Fc was expressed in Expi293 cells as described above. After purification, Mxra8-HRV-Fc was cleaved using HRV 3C protease (Thermo Fisher) at a 1:10 ratio overnight at 4°C . Cleaved Fc fragments were depleted using protein A Sepharose chromatography, and the purity of Mxra8 was confirmed using SDS-PAGE analysis.

Expression of CHIKV VLPs

CHIKV VLPs plasmids (strain 37997) were provided by G. Nabel (Vaccine Research Center, NIH) and expressed in Expi293 cells as previously described¹⁸. The supernatant was harvested four days after transfection, 0.2 μ m filtered, and stored at 4°C .

ELISA-based Mxra8-Fc binding assays

Anti-CHIKV human mAb 4N12¹⁹ or anti-EEEV human mAb 53 (J. Crowe, unpublished data) were immobilized (50 μ l, 2 μ g/ml) onto Maxisorp ELISA plates (Thermo Fisher) overnight in sodium bicarbonate buffer, pH 9.3. Plates were washed four times with PBS and blocked with PBS supplemented with 4% BSA for 1 h at room temperature. CHIKV-181/25 or SINV-EEEV was diluted to 1.5×10^7 FFU/ml in PBS and 50 μ l/well was added for 1 h at

room temperature. Mxra8-Fc and respective positive (CHK-11⁵ and EEEV-10 (A. Kim and M. Diamond, unpublished results) and negative OPC-Fc (D. Fremont, unpublished results) controls were diluted in PBS supplemented with 2% BSA and incubated for 1 h at room temperature. After serial washes with PBS, plates were incubated with horseradish peroxidase conjugated goat anti-mouse IgG (H+L) (1:2000 dilution, Jackson ImmunoResearch) for 1 h at room temperature. After washing with PBS, plates were developed with 3,3',5,5' tetramethylbenzidine substrate (Dako) and 2N H₂SO₄. Absorbance was read at 450 nm with a TriStar Microplate Reader (Berthold). The mAb competition binding assay was performed by incubating 10 µg/ml of indicated anti-CHIKV human mAbs¹⁹ for 30 min prior to the addition of mMxra8-Fc, as described above; the anti-CHIKV human mAbs were mapped previously to different epitopes by alanine scanning mutagenesis and evaluated for neutralizing activity¹⁹. Humanized anti-WNV mAb E16³¹ was included as a negative control in competition binding assays.

Surface plasmon resonance based Mxra8 binding assay

Surface plasmon resonance binding experiments were performed on a Biacore T200 system (GE Healthcare) to measure the kinetics and affinity of Mxra8 binding to CHIKV VLPs. Experiments were performed at 30 µl/min and 25°C using HBS-EP (0.01 M HEPES pH 7.4, 0.15 M NaCl, 3 mM EDTA, 0.005% v/v Surfactant P20) as running buffer. CHK-265 mAb⁵ was immobilized onto a CM5 sensor chip (GE Healthcare) using standard amine coupling chemistry, and CHIKV VLPs were captured. Recombinant Mxra8 was injected over a range of concentrations (1 µM to 20 nM) for 5 min followed by a 10 min dissociation period. As a negative control, murine norovirus was captured with mAb A6.2, as described previously³⁴. Real-time data was analyzed using BIAevaluation 3.1 (GE Healthcare). Kinetic profiles and steady-state equilibrium concentration curves were fitted using a global 1:1 binding algorithm with drifting baseline.

Cell-based Mxra8-Fc binding assay

3T3 cells were inoculated with different viruses at the following MOI: CHIKV-181/25 (MOI of 3, 9.5 h), ONNV (MOI of 5, 12 h), MAYV (MOI of 3, 24 h), RRV (MOI of 3, 32 h), SINV (MOI of 10, 9 h), and VEEV (MOI of 3, 6.5 h). Cells were detached using TrypLE (Thermo Fisher #12605010), washed twice with cold HBSS supplemented with 15 mM HEPES and 2% FBS. Cells were incubated with 1 µg/mL of Mxra8-Fc, OPG-Fc, or viral E2-specific antibodies at 4°C for 25 min. After washing, cells were stained with goat anti-mouse IgG (H+L) conjugated with Alexa Fluor 647 for 25 min at 4°C. After washing twice, cells were fixed with 2% PFA for 10 min at room temperature. After two additional washes, cells were subjected to flow cytometry analysis.

Virus binding and internalization assays

The assays were conducted in suspension. MEFs cells were collected using TrypLE and washed twice with ice-cold medium supplemented with 2% FBS. CHIKV AF15561 virions were purified through a 25% glycerol cushion at 25,000 rpm for 2 h. For the binding assay, cells (5 x 10⁵) and virions (MOI of 20) were mixed in a 1.5-ml microcentrifuge tube and incubated on ice for 45 min. After five cycles of centrifugation and washing, cells were lysed in RLT buffer for RNA extraction using an RNeasy Mini Kit (QIAGEN #74104). For

internalization assay, after 5 cycles of centrifugation and washing, cells were resuspended into medium supplemented with 2% FBS and 15 mM NH₄Cl and then incubated at 37°C for 1 h. Cells were chilled on ice and treated with 500 ng/mL protease K on ice for 1 h. After three additional washes, cells were lysed in RLT buffer for RNA extraction. RT-qPCR was conducted with *Gapdh* as an internal control using a TaqMan™ RNA-to-CT™ 1-Step Kit (Thermo Fisher Scientific #4392938). Primers and probes used are as follows: Fwd-CHK181/AF: 5'-TCGACGCGCCATCTTTAA-3'; Rev-CHK181/AF: 5'-ATCGAATGCACCGCACACT-3'; Probe-CHK181/AF: 5'-6-FAM/ACCAGCCTG/ZEN/CACCCACTCCTCAGAC/3'-IABkFQ; Fwd-Gapdh: 5'-GTGGAGTCATACTGGAACATGTAG-3'; Rev-Gapdh: 5'-AATGGTGAAGGTCGGTGTG-3'; and Probe-Gapdh: 5'-6-FAM/TGCAAATGG/ZEN/CAGCCCTGGTG/3'-IABkFQ.

For the flow cytometry-based binding assay, experiments were conducted as above but with 5 x 10⁴ cells and an MOI of 200. After binding and washing, cells were fixed and stained with a mixture of mAbs (CHK-11, CHK-84, CHK-124, and CHK-166⁵) (1 µg/mL) at room temperature for 25 min. Cells were washed once and stained with 2 µg/mL of goat anti-mouse IgG (H+L) conjugated with Alexa Fluor 647 (Thermo Fisher #A21235) for 25 min. After two additional washes, cells were subjected to flow cytometry analysis.

Surface staining of mouse Mxra8 and human MXRA8

Mouse or human cells were harvested with TrypLE and washed twice with cold Hank's Balanced Salt Solution (HBSS) supplemented with 15 mM HEPES and 2% FBS. Cells were incubated with anti-Mxra8 (mouse) armenian hamster serum (1:300), anti-Mxra8 (mouse) hamster mAbs (1 µg/mL), or anti-MXRA8 (human) mAb (1 µg/mL) (MBL International # W040-3) at 4°C for 25 min. After washing, cells were stained with 2 µg/mL goat anti-Armenian hamster IgG H&L conjugated with Alexa Fluor® 647 (Abcam #ab173004) or goat anti-mouse IgG (H+L) conjugated with Alexa Fluor 647 (Thermo Fisher Scientific #A21235) for 25 min at 4°C. After two additional washes, cells were fixed with 2 % PFA for 10 min at room temperature. Cells were then washed twice and subjected to flow cytometry analysis.

Cell viability assay

A CellTiter-Glo® Luminescent Cell Viability Assay (Promega) was performed according to the manufacturer's instructions. Briefly, 2 x 10⁴ of 3T3 or MEFs cells in 100 µl culture medium were seeded into opaque-walled 96-well plates. 24 h later, 100 µl of CellTiter-Glo® reagent was added to each well and allowed to shake for 2 min. After a 10 min incubation at room temperature for 10 min, luminescence was recorded by using a Synergy H1 Hybrid Plate Reader (Biotek) with an integration time of 0.5 second per well.

Western blotting

Cells seeded in 6-well plates were washed once with PBS, chilled on ice in PBS, and detached with a cell scraper. After spinning at 300 x g for 5 min, cell pellets were lysed in 45 µl RIPA buffer (Cell Signaling #9806S) with a cocktail of protease inhibitors (Sigma-Aldrich # S8830). Samples were prepared in LDS buffer (Life Technologies) under reducing

(+ dithiothreitol) conditions. After heating (70°C, 10 min), samples were electrophoresed using 10% Bis-Tris gels (Life Technologies) and proteins were transferred to PVDF membranes using an iBlot2 Dry Blotting System (Life Technologies). Membranes were blocked with 5% non-fat dry powdered milk and probed with hamster mAb 3G2.F5 (0.5 µg/ml) against mouse Mxra8. Western blots were developed using SuperSignal™ West Pico Chemiluminescent Substrate or SuperSignal™ West Femto Maximum Sensitivity Substrate (Life Technologies).

Alanine scanning mutagenesis for mapping

A CHIKV E2, 6K, and E1 envelope protein expression construct (strain S27, Uniprot Reference #Q8JUX5) with a C-terminal V5 tag was subjected to alanine scanning mutagenesis to generate a comprehensive mutation library³⁵. Each residue of the envelope proteins was mutated to alanine, with alanine codons mutated to serine. 141 mutations within the E2 A and B domains were screened for binding by Mxra8-Fc. Binding of Mxra8-Fc to each mutant expressed in HEK-293T cells was determined by immunofluorescence detected with a high-throughput flow cytometer (Intellicyt), as described previously³⁵. Residues of domains A or B were identified as contributing to the binding site if their mutation eliminated Mxra8-Fc binding, but supported binding of CHIKV mAbs that bind to the appropriate domain (control mAbs were CHV-84, CHKV-88, IM-CHKV063, IM-CKV065, and C9^{5,35,36}).

Mapping of mutations onto the CHIKV p62-E1 crystal structure

Figures were prepared using the atomic coordinates of CHIKV pE2-E1 (RCSB accession number 3N42) using the program PyMOL (The PyMOL Molecular Graphics System, Version 1.7.4 Schrödinger, LLC).

MAB generation

4 week-old male Armenian hamsters were immunized intravenously with 100 µg of purified Mxra8-Fc. After two boosts (~ 7 months of age), spleens were harvested for hybridoma fusion and mAb production. Hybridoma supernatants were initially screened by ELISA using Mxra8-human Fc (mouse Fc was replaced by human Fc). As a second assay, we examined the binding of hybridoma supernatants to Mxra8 on the surface of 3T3 cells by flow cytometry. Finally, a tertiary screen evaluating blockade of CHIKV-181/25 infection by hybridoma supernatants was performed in 3T3 cells. After limiting dilution subcloning, the seven clones with the strongest blocking activities were selected and expanded. Antibodies were purified using protein A-Sepharose™ 4B (Invitrogen #101042), dialyzed in PBS, concentrated, and filtered for *in vitro* and *in vivo* experiments.

Blocking assays with Mxra8-Fc, MXRA8-2-Fc, or anti-Mxra8 mAbs

2.5×10^4 of 3T3 or MRC-5 cells were seeded into 96-well plates 12 h prior to treatment. CHIKV-181/25 virions were purified through a 25% glycerol cushion at 25,000 rpm for 2 h. Serially diluted Mxra8-Fc or MXRA8-2-Fc protein was incubated with purified virions (MOI of 3) for 1 h at 37°C in a volume of 100 µl. The mixture was added to 3T3 or MRC-5 cells for 9.5 h or 11.5 h, respectively. Cells were then harvested for intracellular E2

expression as measured by flow cytometry. For hamster mAb blocking experiments, 3T3 or MRC-5 cells were pre-incubated with serially diluted mAbs for 1 h at 37°C in a volume of 50 µl, and then purified virions (MOI of 3) in 50 µl were added and incubated for 9.5 or 11.5 h, respectively. Cells were harvested and intracellular E2 expression was analyzed by flow cytometry. For hamster mAb blocking experiments on primary human cells (KE, DF, SF, OB, CH, and SMC), 2×10^4 of cells were seeded into 96-well plates 12 h prior to treatment. Cells were pre-incubated with Armenian hamster isotype control (Bio X Cell # BE0260), 1H1.F5, or 9G2.D6 mAb for 1 h at 37°C in a volume of 50 µl (50 µg/ml), and subsequently, purified CHIKV-AF15561 virions (MOI of 15) in 50 µl were added and incubated for 10.5 h. Cells were harvested and intracellular E2 expression was analyzed by flow cytometry.

PI-PLC treatment

3T3 cells (10^5) expressing GPI-anchored Mxra8 were harvested using TrypLE and washed twice with PBS. Cells were then treated with 1 U/mL of phosphatidylinositol-specific phospholipase C (PI-PLC) (Sigma-Aldrich #P8804) in 50 µl PBS at 37°C for 1 h. After two more cycles of washing, cells were stained for Mxra8 expression and processed by flow cytometry analysis as described above.

Mouse experiments

Experiments were carried out in accordance with the recommendations in the Guide for the Care and Use of Laboratory Animals of the National Institutes of Health after approval by the Institutional Animal Care and Use Committee at the Washington University School of Medicine (Assurance number A3381-01). Mxra8-Fc or an IgG control (JEV-13 mAb) (250 µg per mouse in PBS) was administered to four week-old WT male C57BL/6J mice 6 h prior to subcutaneous inoculation in the footpad with 10^3 FFU of CHIKV-AF15561. Alternatively, in co-injection experiments, CHIKV or ONNV was mixed directly with Mxra8-Fc or JEV-13 (25 µg per mouse in PBS), and incubated at 37°C for 30 min before inoculation. At 12 h, 24 h, and 72 h post infection, animals were euthanized, and after perfusion with PBS, indicated tissues were harvested. For antibody pre- or post-treatment experiments, 300 µg of purified hamster mAbs 1G11.E6 + 7F1.D8, 4E7.D10 + 8F7.E1, and isotype control PIP (Bio X cell # BE0260) in PBS were administered via an intraperitoneal route to four week-old WT male C57BL/6 mice 12 h prior or 8 or 24 h post subcutaneous inoculation in the footpad with 10^3 FFU of CHIKV AF15561. Virus was titrated by FFA as described⁵ using mouse CHK-11⁵ for CHIKV or mouse CHK-48 for ONNV as the detection antibody. Joint swelling was monitored at 72 h post infection via left foot measurements (width x height) using digital calipers as described previously³⁷. Samples sizes were estimated to determine a difference of 3 to 5-fold, depending on data distribution. Blinding and randomization were not performed.

Statistical analysis

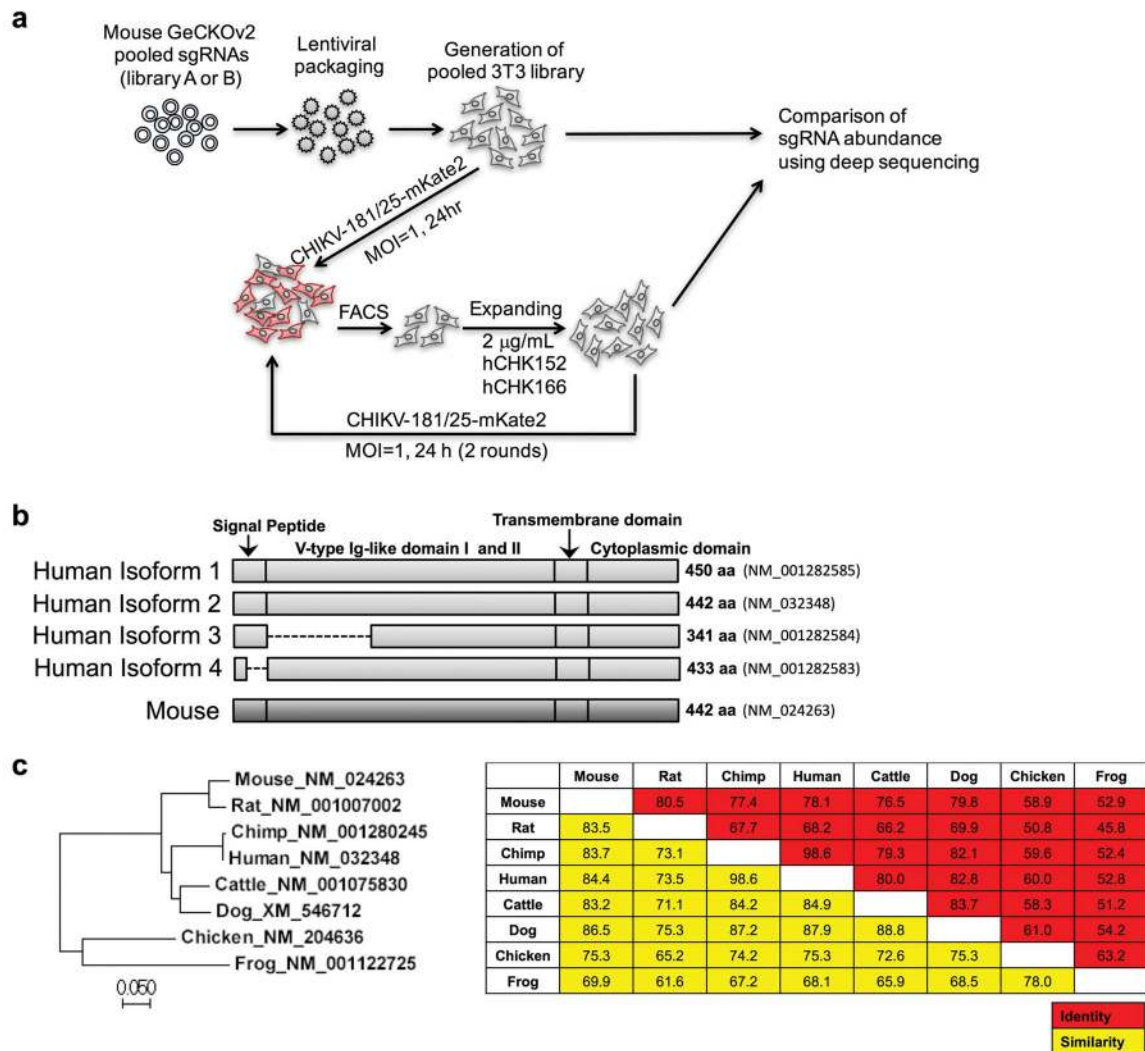
Statistical significance was assigned when *P* values were < 0.05 using Prism Version 7 (GraphPad). Cell culture experiments were analyzed by multiple t-tests with a Holm-Sidak correction or ANOVA with a multiple comparison correction. Analysis of levels of joint swelling or viral burden *in vivo* was determined by a Mann-Whitney, ANOVA, Kruskal

Wallis, or unpaired t-test depending on data distribution and the number of comparison groups.

Data Availability

The authors declare that all data supporting the findings of this study are available within the paper and its Supplementary information. The Supplemental Tables provide data for the CRISPR-Cas9 screen, statistical analysis, and alanine scanning mutagenesis mapping of the Mxra8-Fc binding site on CHIKV.

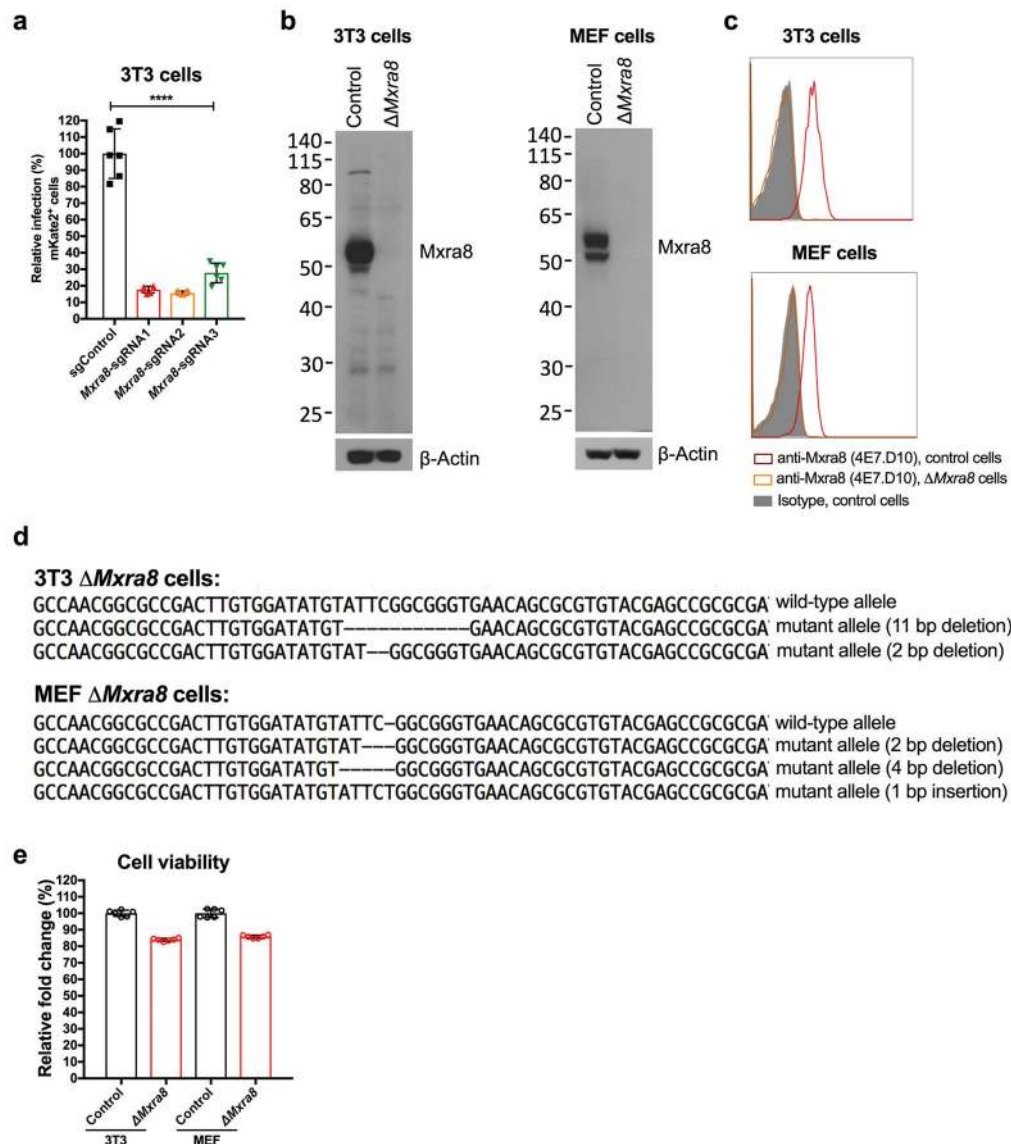
Extended Data



Extended Data Figure 1. RISPR-Cas9-based gene editing screen

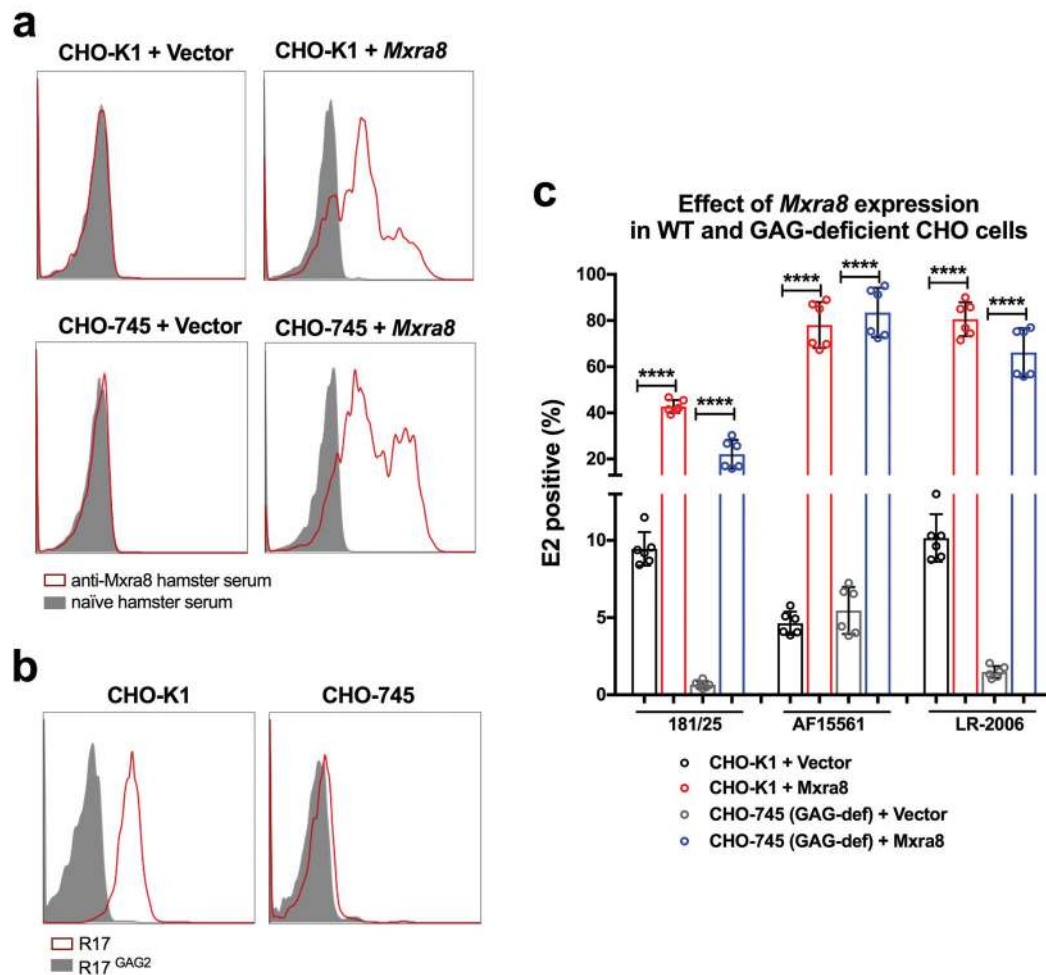
Mouse 3T3 cells were transduced separately with two half libraries (A + B) comprising 130,209 sgRNAs, selected with puromycin, and then inoculated with CHIKV-181/25-mKate2 (MOI of 1). One day later, mKate2-negative cells were sorted, and expanded in the presence of 2 µg/ml each of CHK-152 and CHK-166 neutralizing mAbs. Several days later,

cells were re-inoculated with CHIKV-181/25-mKate2 without neutralizing mAbs and re-sorted for mKate2-negative cells. This procedure was repeated one additional time. Afterwards, genomic DNA was harvested for sgRNA sequencing and compared to the parent library for abundance (see Supplemental Tables 1 and 2). **b.** Diagram of the mouse *Mxra8* and human *MXRA8* orthologs. The transcript identification numbers and length of proteins are indicated to the right. Partial deletions in the isoforms 3 and 4 are shown as dashed lines. **c.** Phylogenetic tree of *Mxra8* indicating genetic relationships. The Neighbor-Joining tree was constructed using MEGA 7. Scale bar shows the branch length. (*Right*) Identity (red) and similarity (yellow) matrix indicating the conservation of *Mxra8* between species. The matrix was generated using MagGat 1.8.



Extended Data Figure 2. Efficiency of targeting *Mxra8* expression by CRISPR-Cas9 gene editing
a. 3T3 cells were edited with a control or three different *Mxra8* sgRNAs. After puromycin selection, bulk cells were inoculated with chimeric CHIKV-181/25-mKate2 and processed

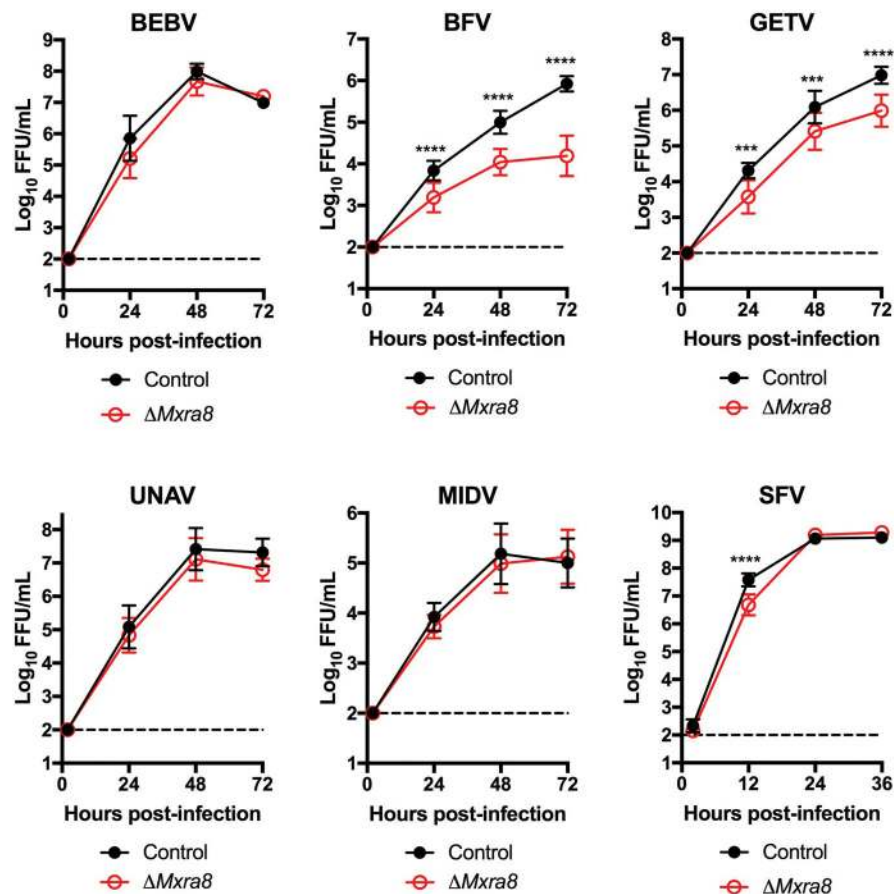
for marker gene expression by flow cytometry. Data are pooled from three experiments and expressed as mean \pm SD ($n = 6$, one-way ANOVA with a Dunnett's multiple comparison test compared to control, ****, $P < 0.0001$). **b.** Western blotting of Mxra8 in control and $\Delta Mxra8$ 3T3 or MEF cells using hamster mAb 3G2.F5. One representative of two is shown. **c.** 3T3 and MEF cells (parent or $\Delta Mxra8$) were tested for Mxra8 surface expression by flow cytometry using anti-Mxra8 antibody (4E7.D10) and an isotype control mAb. One representative experiment of two is shown. **d.** Sanger sequencing of Mxra8 in control and $\Delta Mxra8$ 3T3 or MEF cells. Sequencing data shows an alignment and individual out-of-frame deletions. **e.** Viability of control and $\Delta Mxra8$ 3T3 and MEF cells. An equal number of cells were plated and viability was assessed over a 24 h period using the Cell-Titer Glo assay. The results were normalized to control cells and pooled from two experiments ($n = 6$). Error bars indicate SD.



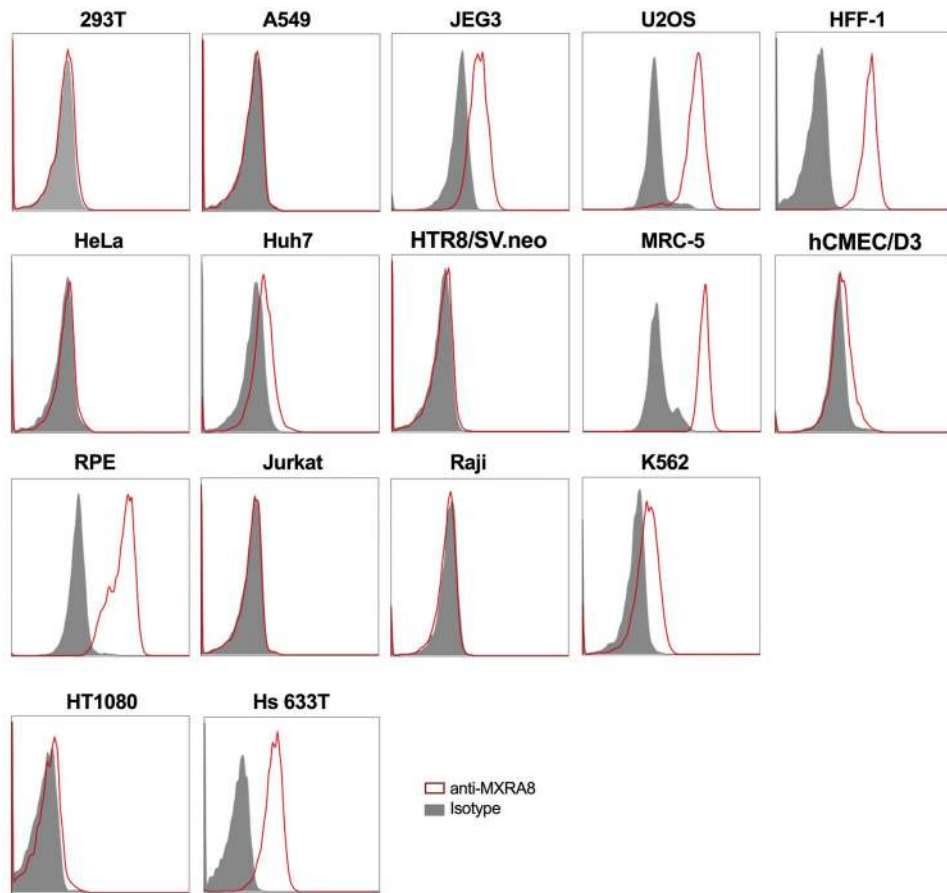
Extended Data Figure 3. CHIKV infectivity in CHO-K1 and CHO-745 cells in the presence or absence of ectopic Mxra8 expression

a. Surface expression of Mxra8 on CHO-K1 (WT) and CHO-745 (glycosaminoglycan deficient¹⁵) cells stably transduced with control (vector-only) or mouse Mxra8 as judged by flow cytometry. **b.** Confirmation of HS expression on the surface of CHO-K1 (WT) and

CHO-745 cells. Surface expression of HS was evaluated using the R17 protein of rodent herpesvirus Peru, which binds to glycosaminoglycans on the surface of cells³⁸. R17^{GAG2} is a mutant form of the protein that lacks binding to glycosaminoglycans and served as a negative control. For **a** and **b**, data are representative of two experiments. **c**. CHO-K1 (WT) and CHO-745 cells were transduced stably with control (vector) or mouse Mxra8 and inoculated with CHIKV (strains 181/25, AF15561, or LR-2006) and processed for intracellular E2 protein staining by flow cytometry. Data are from three experiments: mean \pm SD (n = 6, one-way ANOVA with a Dunnett's multiple comparison test, ****, $P < 0.001$).

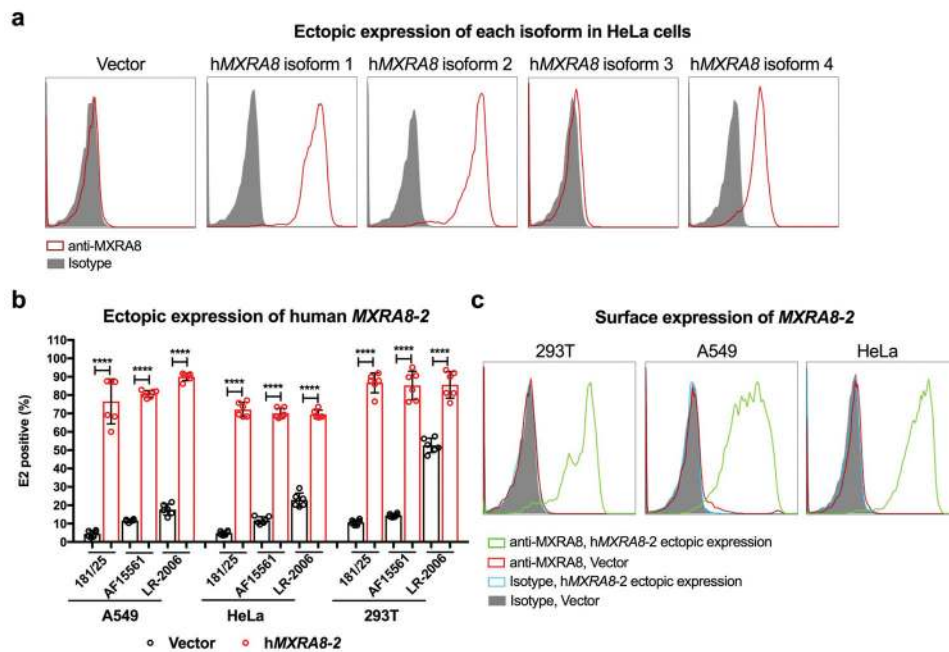


Extended Data Figure 4. Growth curves of related alphaviruses in Δ Mxra8 3T3 cells
Control and Δ Mxra8 3T3 cells were inoculated with Bebaru (BEBV), Barmah Forest (BFV), Getah (GETV), Una (UNAV), Middleburg (MIDV), or Semliki Forest (SFV) viruses at an MOI of 0.01 (except for BEBV, which was at 0.001), and supernatants were harvested at the indicated times for FFA. Data are pooled from two (BEBV) or three (all others) experiments and expressed as mean \pm SD (n = 6, BEBV; n = 9, BFV, GETV, UNAV, and MIDV; n = 12, SFV; two-way ANOVA with Sidak's multiple comparisons test, ***, $P < 0.001$; ****, $P < 0.0001$).



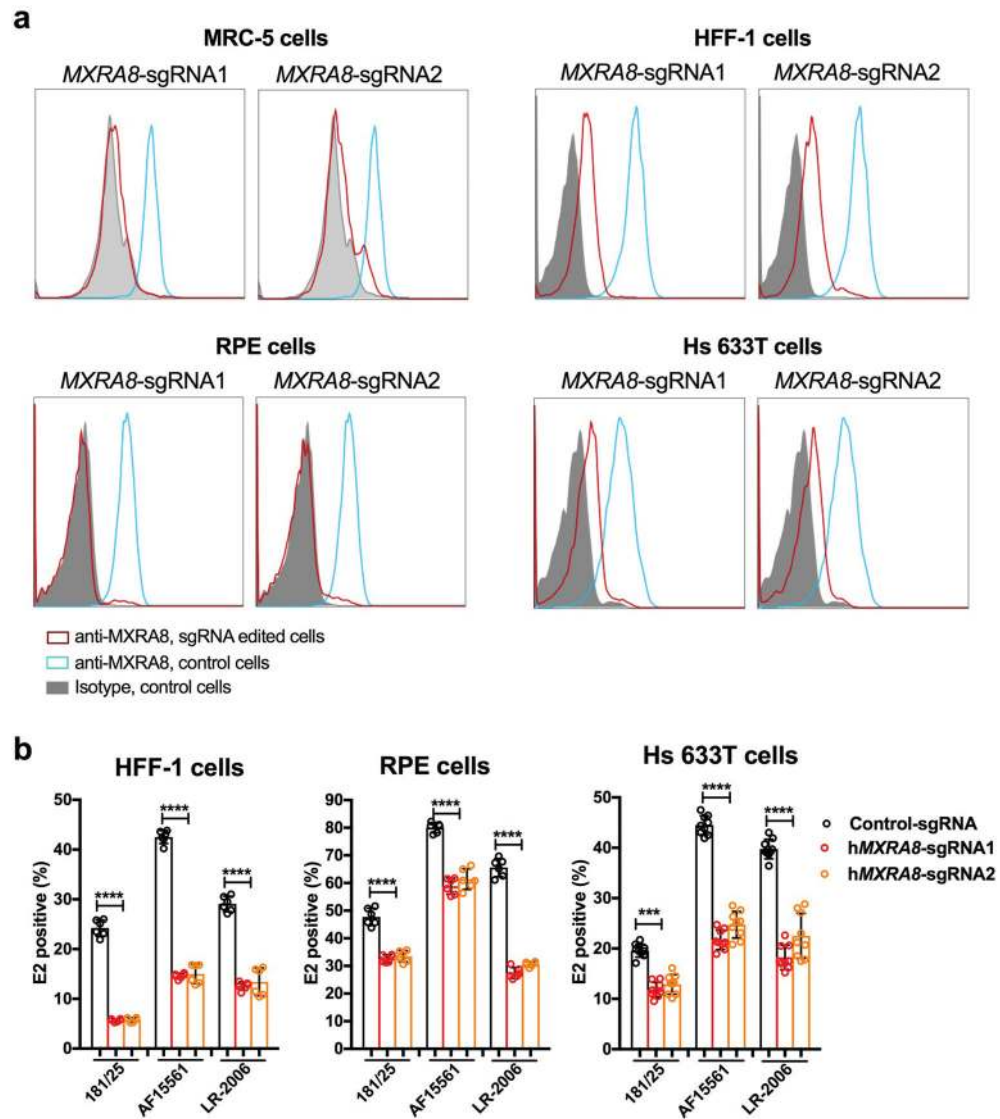
Extended Data Figure 5. Surface expression of MXRA8 in different human cell lines

Human cell lines were tested for MXRA8 surface expression by flow cytometry: 293T (embryonic kidney), A549 (lung adenocarcinoma), JEG3 (placental choriocarcinoma), U2OS (osteosarcoma), HFF-1 (foreskin fibroblasts), HeLa (cervical carcinoma), Huh7 (hepatocarcinoma), HTR8/SV.neo (trophoblast progenitor), MRC-5 (lung carcinoma), hCMEC/D3 (cerebral microvascular endothelial cells), RPE (retinal pigment epithelial cell), Jurkat (T cell lymphoma), Raji (B cell lymphoma), K562 (erythroleukemia), HT1080 (fibrosarcoma), and Hs 633T (fibrosarcoma) cells. Representative data are shown of two independent experiments. Gray histograms, isotype control mAb; red histograms, anti-MXRA8 mAb.



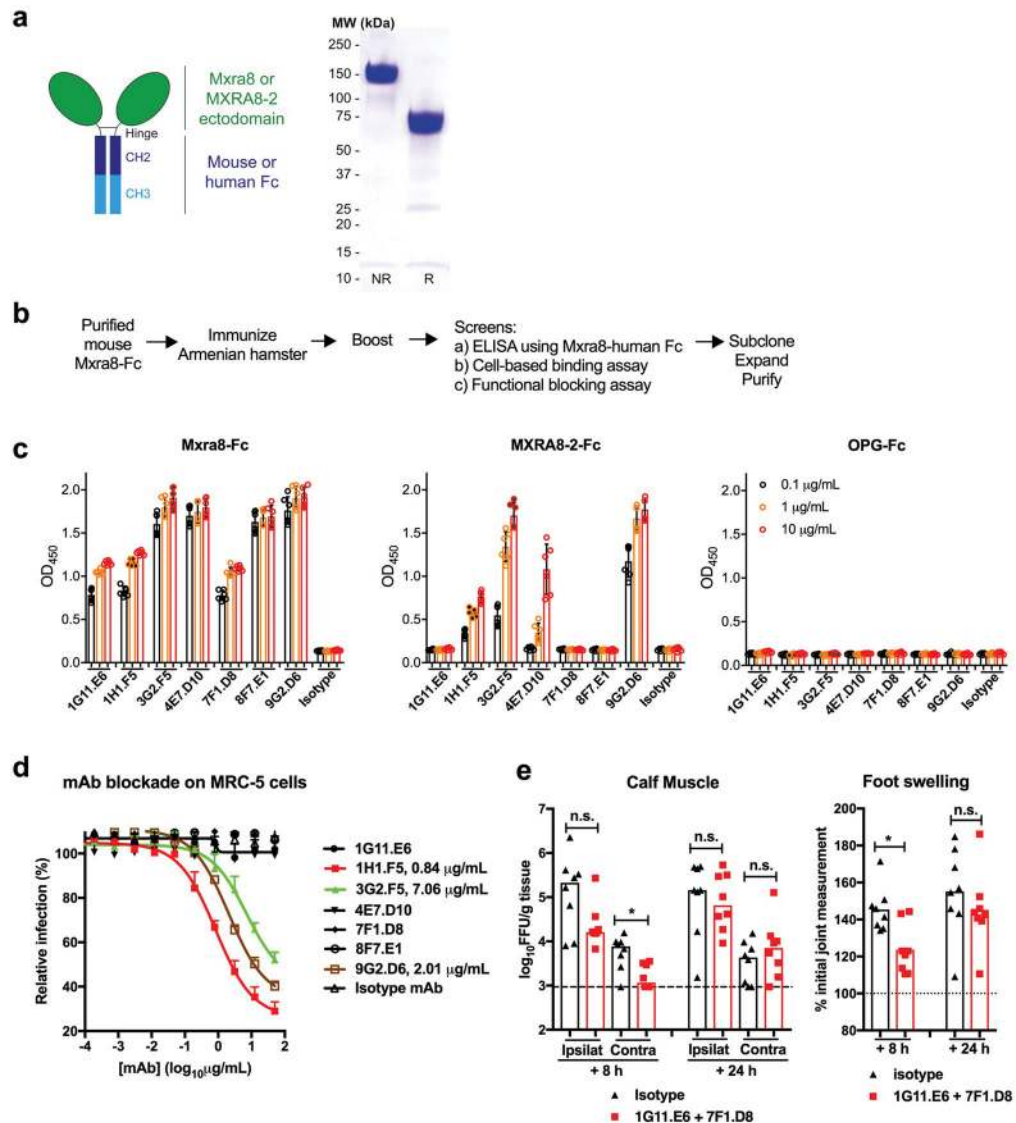
Extended Data Figure 6. MXRA8 supports enhanced infection of different CHIKV strains

a. Transduction and expression of different *MXRA8* (-1, -2, -3, and -4) isoforms in HeLa cells. Representative data is shown from two experiments. Gray histograms, isotype control mAb; red histograms, anti-MXRA8 mAb. **b.** Effect of ectopic expression of *MXRA8-2* on CHIKV (181/25, AF15561, and LR-2006) infection of A549, HeLa, or 293T cells. Cells were harvested and stained for CHIKV antigen with an anti-E2 antibody. Data are pooled from three experiments and expressed as mean \pm SD. Asterisks indicate statistical significance ($n = 6$; two-tailed t-test with Holm-Sidak multiple comparison correction, ***, $P < 0.001$; ****, $P < 0.0001$). **c.** Transduction and expression of *MXRA8-2* in 293T, A549, and HeLa cells. Representative data is shown from two experiments.



Extended Data Figure 7. Gene-editing of MXRA8 in human cell lines

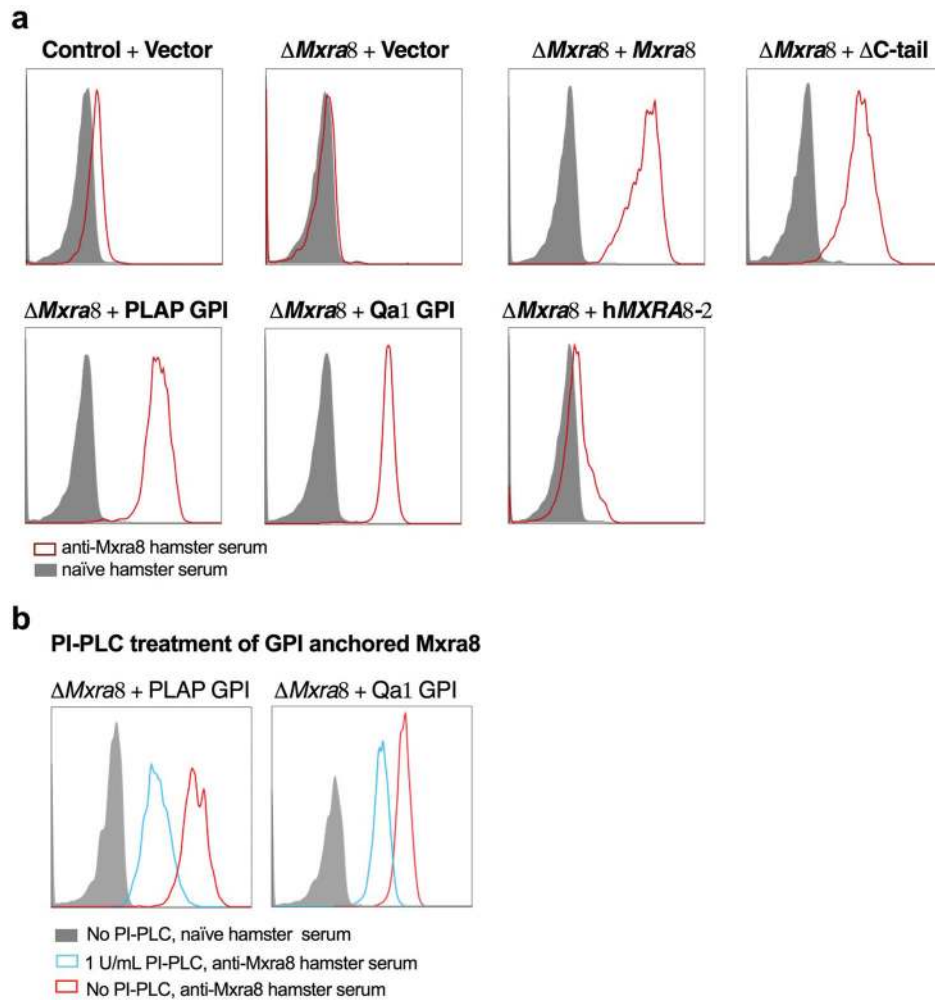
a. Flow cytometry analysis of MXRA8 expression in human MRC-5, HFF-1, RPE, and Hs 633T cells expressing control or two different MXRA8 sgRNAs. Data are representative of two experiments. **b.** Gene-edited cells were inoculated with CHIKV (181/25, AF15561, or LR-2006) in HFF-1, RPE, and Hs 633T cells. Cells were stained for viral antigen with an anti-E2 antibody. Data are pooled from two (HFF-1 and Hs 633T) or three (RPE) independent experiments and expressed as mean values \pm SD ($n = 6$; one-way ANOVA with a Dunnett's multiple comparison test compared to the control, ****, $P < 0.0001$).



Extended Data Figure 8. Mxra8-Fc and anti-Mxra8 generation and function

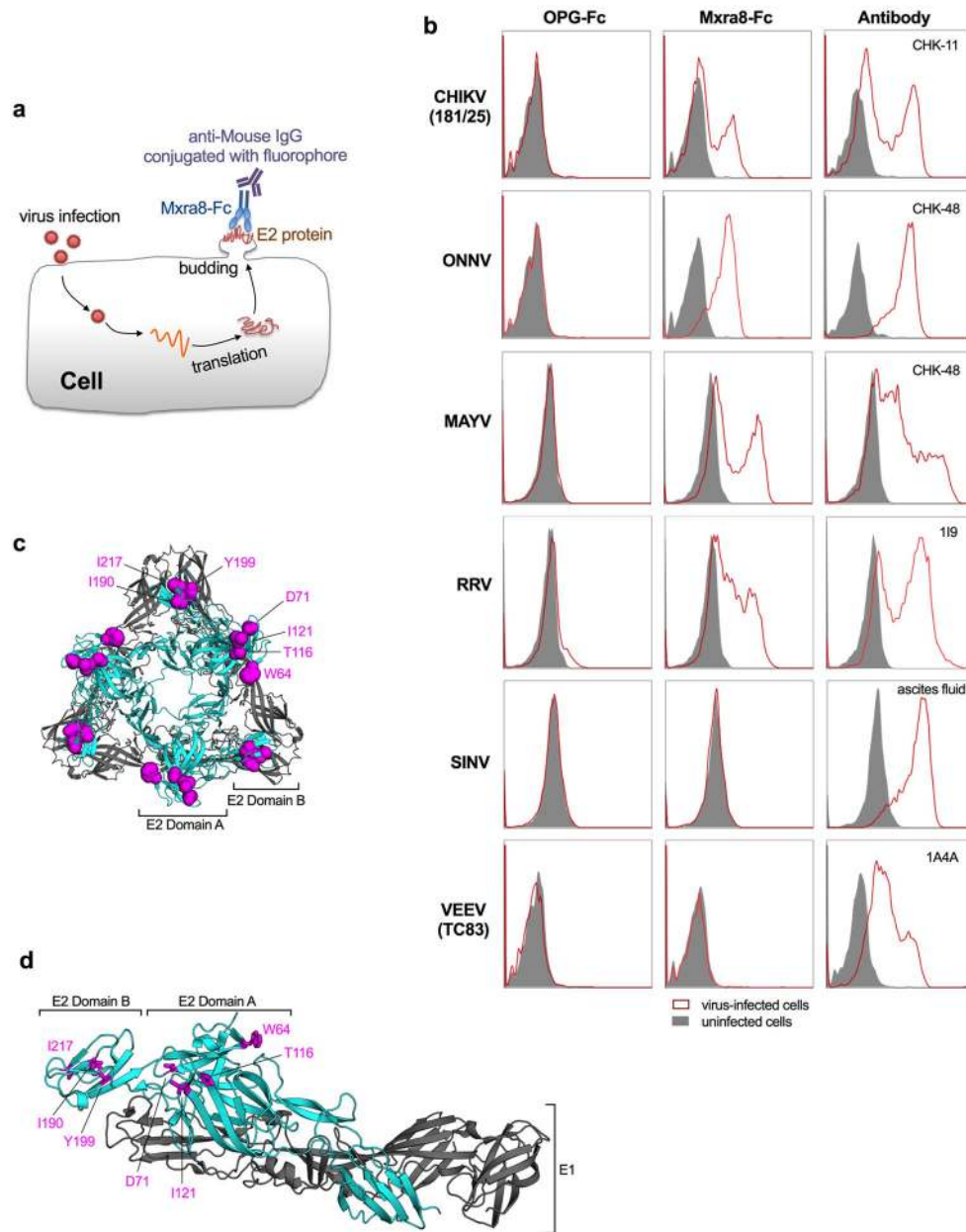
a. Diagram of Mxra8-Fc (*left*) and SDS-PAGE (non-reducing [NR] and reducing [R] conditions) of purified material (*right*). Data are representative of three experiments. **b.** Scheme of anti-Mxra8 generation in Armenian hamsters. **c.** ELISA reactivity of anti-Mxra8 mAbs against Mxra8-Fc, MXRA8-2-Fc, or OPG-Fc. Purified proteins (50 μl, 5 μg/ml) were immobilized overnight at 4°C on ELISA plates. Anti-Mxra8 and isotype control mAbs were incubated for 1 h at room temperature. Signal was detected at 450 nm after incubation with horseradish peroxidase conjugated goat anti-Armenian hamster IgG (H+L) and development with 3,3'-5,5' tetramethylbenzidine substrate. **d.** Blockade of CHIKV-181/25 infection in MRC-5 cells with seven different hamster anti-Mxra8 or isotype control mAbs. MAbs were pre-incubated with cells for 1 h at 37°C prior to addition of virus. After infection, cells were processed for E2 staining by flow cytometry. Relative infection was compared to a no mAb condition using flow cytometry and anti-E2 staining. Data in **c** and **d** are pooled from two experiments (n = 6) and expressed as mean ± SD. **e.** Anti-Mxra8 mAbs (1G11 + 7F1) or

isotype control hamster mAbs (300 μ g total) were administered via intraperitoneal route 8 or 24 hours after inoculation of CHIKV-AF15561 in the footpad. (*Left*) At 72 h after initial infection, CHIKV titers were measured in the ipsilateral and contralateral gastrocnemius (calf) muscles. (*Right*) At 72 h, ipsilateral foot swelling was measured and compared to measurements taken immediately prior to infection. Data are pooled from two experiments ($n = 8$; *, $P < 0.05$; two-tailed Mann-Whitney test) and expressed as median values.



Extended Data Figure 9. Expression of truncated forms of Mxra8 mutants

a. Cell surface expression of Mxra8 in $\Delta Mxra8$ 3T3 cells trans-complemented with vector, *Mxra8*, *Mxra8* ΔC -tail, *Mxra8* with GPI anchors (PLAP or Qa1-derived), or *MXRA8-2*. Data are representative of two independent experiments. Gray histograms, isotype control mAb; red histograms, anti-Mxra8 mAb. **b.** Effect of PI-PLC treatment on expression of different GPI anchored (PLAP or Qa1-derived) forms of Mxra8. Data are representative of two independent experiments. Gray histograms, isotype control mAb; red histograms, untreated, anti-Mxra8 mAb; blue histograms, PI-PLC-treated, anti-Mxra8 mAb.



Extended Data Figure 10. Binding of Mxra8-Fc to surface-displayed E2 protein in virus-infected cells

a. Diagram of the cell-based binding assay. After infection, viral structural proteins (*e.g.*, E2) traffic to the cell plasma membrane where progeny virion assembles and buds. E2 protein is displayed on the cell surface and is accessible to the binding of Mxra8-Fc and detection with a goat anti-mouse IgG secondary antibody by flow cytometry. **b.** Binding of Mxra8-Fc to virus-infected WT 3T3 cells. Cells were infected with the indicated viruses and processed for Mxra8-Fc binding by flow cytometry. Virus-specific anti-E2 Abs were used as positive controls. Data are representative of two independent experiments. **c–d.** Mapped residues by are shown as magenta spheres (**c**) or sticks (**d**) on the CHIKV p62-E1 structure

(**c**, trimer of dimers, top view; **d**, heterodimer, side view) using PyMOL (PDB 3N41). The E1 and E2 proteins are colored in grey and cyan, respectively.

Supplementary Material

Refer to Web version on PubMed Central for supplementary material.

Acknowledgments

This study was supported by NIH grants R01AI114816, R01AI123348, and R01AI095436, contract HHSN272201400058C, and the Defense Reduction Threat Agency HDTRA1-15-1-0013. We thank Mark Heise, Thomas Morrison, Michael Farzan, Jonathan Miner, and Terence Dermody for discussions, reagents, and comments on the manuscript.

References

1. Weaver SC, Charlier C, Vasilakis N, Lecuit M. Zika, Chikungunya, and Other Emerging Vector-Borne Viral Diseases. *Annual review of medicine*. 2017
2. Vancini R, Hernandez R, Brown D. Alphavirus entry into host cells. *Progress in molecular biology and translational science*. 2015; 129:33–62. DOI: 10.1016/bs.pmbts.2014.10.002 [PubMed: 25595800]
3. Cong L, et al. Multiplex genome engineering using CRISPR/Cas systems. *Science*. 2013; 339:819–823. science.1231143 [pii]. DOI: 10.1126/science.1231143 [PubMed: 23287718]
4. Jinek M, et al. RNA-programmed genome editing in human cells. *eLife*. 2013; 2:e00471. [pii]. [PubMed: 23386978]
5. Pal P, et al. Development of a highly protective combination monoclonal antibody therapy against Chikungunya virus. *PLoS Pathog*. 2013; 9:e1003312. [PubMed: 23637602]
6. Li W, et al. MAGeCK enables robust identification of essential genes from genome-scale CRISPR/Cas9 knockout screens. *Genome Biol*. 2014; 15:554. s13059-014-0554-4 [pii]. [PubMed: 25476604]
7. Han SW, et al. DICAM inhibits angiogenesis via suppression of AKT and p38 MAP kinase signalling. *Cardiovascular research*. 2013; 98:73–82. DOI: 10.1093/cvr/cvt019 [PubMed: 23386276]
8. Jung YK, et al. DICAM inhibits osteoclast differentiation through attenuation of the integrin alphaVbeta3 pathway. *Journal of bone and mineral research : the official journal of the American Society for Bone and Mineral Research*. 2012; 27:2024–2034. DOI: 10.1002/jbmr.1632
9. Jung YK, et al. DICAM, a novel dual immunoglobulin domain containing cell adhesion molecule interacts with alphavbeta3 integrin. *Journal of cellular physiology*. 2008; 216:603–614. DOI: 10.1002/jcp.21438 [PubMed: 18366072]
10. Yonezawa T, et al. Limitrin, a novel immunoglobulin superfamily protein localized to glia limitans formed by astrocyte endfeet. *Glia*. 2003; 44:190–204. DOI: 10.1002/glia.10279 [PubMed: 14603461]
11. Barton ES, et al. Junction adhesion molecule is a receptor for reovirus. *Cell*. 2001; 104:441–451. [PubMed: 11239401]
12. Levitt NH, et al. Development of an attenuated strain of chikungunya virus for use in vaccine production. *Vaccine*. 1986; 4:157–162. [PubMed: 3020820]
13. Gardner CL, Burke CW, Higgs ST, Klimstra WB, Ryman KD. Interferon-alpha/beta deficiency greatly exacerbates arthritogenic disease in mice infected with wild-type chikungunya virus but not with the cell culture-adapted live-attenuated 181/25 vaccine candidate. *Virology*. 2012; 425:103–112. S0042-6822(12)00005-0 [pii]. DOI: 10.1016/j.virol.2011.12.020 [PubMed: 22305131]
14. Ashbrook AW, et al. Residue 82 of the Chikungunya virus E2 attachment protein modulates viral dissemination and arthritis in mice. *J Virol*. 2014; 88:12180–12192. DOI: 10.1128/jvi.01672-14 [PubMed: 25142598]

15. Esko JD, Stewart TE, Taylor WH. Animal cell mutants defective in glycosaminoglycan biosynthesis. *Proc Natl Acad Sci U S A*. 1985; 82:3197–3201. [PubMed: 3858816]
16. Lee J, et al. Structure of the Ebola virus envelope protein MPER/TM domain and its interaction with the fusion loop explains their fusion activity. *Proc Natl Acad Sci U S A*. 2017; 114:E7987–e7996. DOI: 10.1073/pnas.1708052114 [PubMed: 28874543]
17. Doranz BJ, Berson JF, Rucker J, Doms RW. Chemokine receptors as fusion cofactors for human immunodeficiency virus type 1 (HIV-1). *Immunol Res*. 1997; 16:15–28. DOI: 10.1007/bf02786321 [PubMed: 9048206]
18. Akahata W, et al. A virus-like particle vaccine for epidemic Chikungunya virus protects nonhuman primates against infection. *Nat Med*. 2010; 16:334–338. nm.2105 [pii]. DOI: 10.1038/nm.2105 [PubMed: 20111039]
19. Smith SA, et al. Isolation and Characterization of Broad and Ultrapotent Human Monoclonal Antibodies with Therapeutic Activity against Chikungunya Virus. *Cell Host Microbe*. 2015; 18:86–95. S1931-3128(15)00257-7 [pii]. DOI: 10.1016/j.chom.2015.06.009 [PubMed: 26159721]
20. Fox JM, et al. Broadly Neutralizing Alphavirus Antibodies Bind an Epitope on E2 and Inhibit Entry and Egress. *Cell*. 2015; 163:1095–1107. DOI: 10.1016/j.cell.2015.10.050 [PubMed: 26553503]
21. Sun S, et al. Structural analyses at pseudo atomic resolution of Chikungunya virus antibody neutralization mechanisms. *eLife*. 2013; 2:e00435. [PubMed: 23577234]
22. Li L, Jose J, Xiang Y, Kuhn RJ, Rossmann MG. Structural changes of envelope proteins during alphavirus fusion. *Nature*. 2010; 468:705–708. nature09546 [pii]. DOI: 10.1038/nature09546 [PubMed: 21124457]
23. Voss JE, et al. Glycoprotein organization of Chikungunya virus particles revealed by X-ray crystallography. *Nature*. 2010; 468:709–712. nature09555 [pii]. DOI: 10.1038/nature09555 [PubMed: 21124458]
24. Couderc T, Lecuit M. Chikungunya virus pathogenesis: From bedside to bench. *Antiviral Res*. 2015; 121:120–131. DOI: 10.1016/j.antiviral.2015.07.002 [PubMed: 26159730]
25. Rose PP, et al. Natural resistance-associated macrophage protein is a cellular receptor for sindbis virus in both insect and mammalian hosts. *Cell Host Microbe*. 2011; 10:97–104. S1931-3128(11)00218-6 [pii]. DOI: 10.1016/j.chom.2011.06.009 [PubMed: 21843867]
26. Klimstra WB, Ryman KD, Johnston RE. Adaptation of Sindbis virus to BHK cells selects for use of heparan sulfate as an attachment receptor. *Journal of Virology*. 1998; 72:7357–7366. [PubMed: 9696832]
27. Brien JD, Lazear HM, Diamond MS. Propagation, quantification, detection, and storage of West Nile virus. *Curr Protoc Microbiol*. 2013; 31:15D 13 11–15D 13 18. DOI: 10.1002/9780471729259.mc15d03s31
28. Sanjana NE, Shalem O, Zhang F. Improved vectors and genome-wide libraries for CRISPR screening. *Nat Methods*. 2014; 11:783–784. nmeth.3047 [pii]. DOI: 10.1038/nmeth.3047 [PubMed: 25075903]
29. Joung J, et al. Genome-scale CRISPR-Cas9 knockout and transcriptional activation screening. *Nat Protoc*. 2017; 12:828–863. DOI: 10.1038/nprot.2017.016 [PubMed: 28333914]
30. Shalem O, et al. Genome-scale CRISPR-Cas9 knockout screening in human cells. *Science*. 2014; 343:84–87. science.1247005 [pii]. DOI: 10.1126/science.1247005 [PubMed: 24336571]
31. Oliphant T, et al. Development of a humanized monoclonal antibody with therapeutic potential against West Nile virus. *Nature Medicine*. 2005; 11:522–530.
32. Huang IC, et al. SARS coronavirus, but not human coronavirus NL63, utilizes cathepsin L to infect ACE2-expressing cells. *J Biol Chem*. 2006; 281:3198–3203. M508381200 [pii]. DOI: 10.1074/jbc.M508381200 [PubMed: 16339146]
33. Jemielity S, et al. TIM-family proteins promote infection of multiple enveloped viruses through virion-associated phosphatidylserine. *PLoS Pathog*. 2013; 9:e1003232. [PubMed: 23555248]
34. Taube S, et al. High-resolution x-ray structure and functional analysis of the murine norovirus 1 capsid protein protruding domain. *J Virol*. 2010; 84:5695–5705. DOI: 10.1128/jvi.00316-10 [PubMed: 20335262]

35. Selvarajah S, et al. A neutralizing monoclonal antibody targeting the acid-sensitive region in chikungunya virus E2 protects from disease. *PLoS neglected tropical diseases*. 2013; 7:e2423. PNTD-D-13-00600 [pii]. [PubMed: 24069479]
36. Jin J, et al. Neutralizing Monoclonal Antibodies Block Chikungunya Virus Entry and Release by Targeting an Epitope Critical to Viral Pathogenesis. *Cell Rep*. 2015; 13:2553–2564. DOI: 10.1016/j.celrep.2015.11.043 [PubMed: 26686638]
37. Hawman DW, et al. Chronic joint disease caused by persistent chikungunya virus infection is controlled by the adaptive immune response. *J Virol*. 2013; 87:13878–13888. JVI.02666-13 [pii]. DOI: 10.1128/JVI.02666-13 [PubMed: 24131709]
38. Lubman OY, et al. Rodent herpesvirus Peru encodes a secreted chemokine decoy receptor. *J Virol*. 2014; 88:538–546. DOI: 10.1128/jvi.02729-13 [PubMed: 24173234]

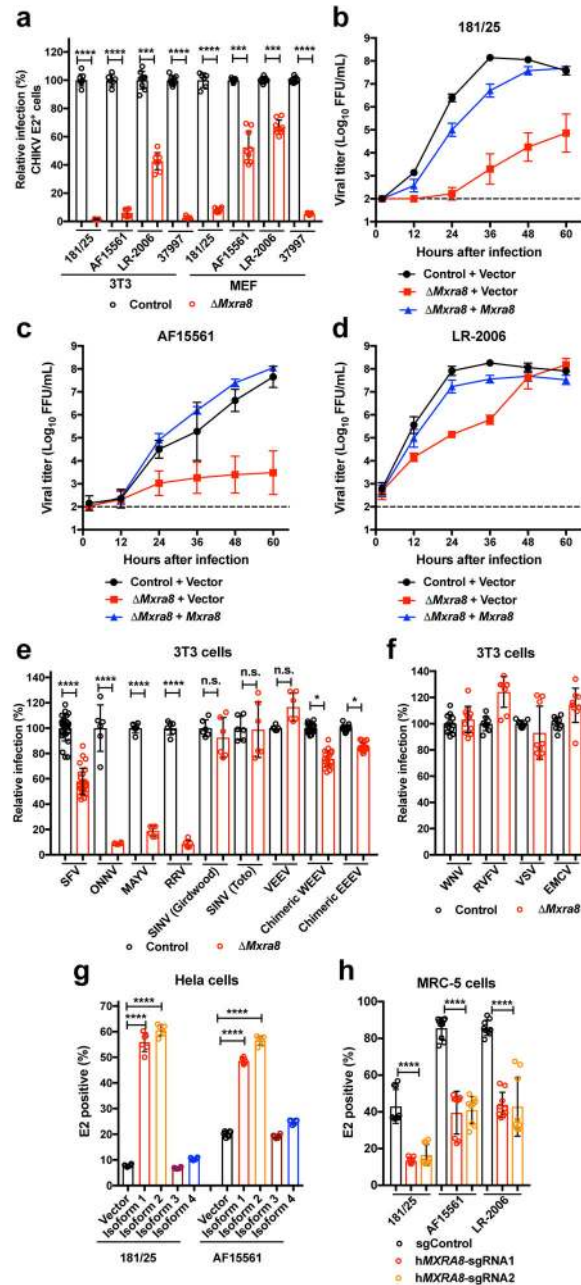


Figure 1. Mxra8 is required for optimal infection of CHIKV and other alphaviruses
a. $\Delta Mxra8$ or control 3T3 or MEF cells were inoculated with CHIKV and stained for E2 protein (3 experiments, $n = 9$; two-tailed t-test with Holm-Sidak correction, ***, $P < 0.001$; ****, $P < 0.0001$; mean \pm standard deviations (SD)). **b–d.** Multi-step growth curves with CHIKV-181/25 (**b**), CHIKV-AF15561 (**c**), or CHIKV-LR-2006 (**d**) in control, $\Delta Mxra8$, or *Mxra8* trans-complemented 3T3 cells (3 experiments, $n = 9$; mean \pm SD). **e.** $\Delta Mxra8$ or control 3T3 cells were inoculated with alphaviruses and processed for E2 or reporter gene expression (3 or more experiments, $n = 6$ except for SFV, WEEV, and EEEV where $n = 18$; two-tailed t-test with Holm-Sidak correction, *, $P < 0.05$; ****, $P < 0.0001$; mean \pm SD). **f.**

$\Delta Mxra8$ or control 3T3 cells were inoculated with indicated viruses and processed for viral antigen or reporter gene expression (3 experiments, mean \pm SD). **g.** HeLa cells were transduced with control or *MXRA8-1*, *-2*, *-3*, or *-4* alleles, inoculated with CHIKV, and processed for E2 staining (3 experiments, n = 6; one-way ANOVA with Dunnett's test, *, $P < 0.05$; **, $P < 0.01$; ***, $P < 0.001$; mean \pm SD). **h.** Human MRC-5 cells depleted of *MXRA8* with two different sgRNA were inoculated with CHIKV, and E2 expression was analyzed (3 experiments, n = 9; one-way ANOVA with Dunnett's test, ****, $P < 0.0001$; mean \pm SD).

Author Manuscript

Author Manuscript

Author Manuscript

Author Manuscript

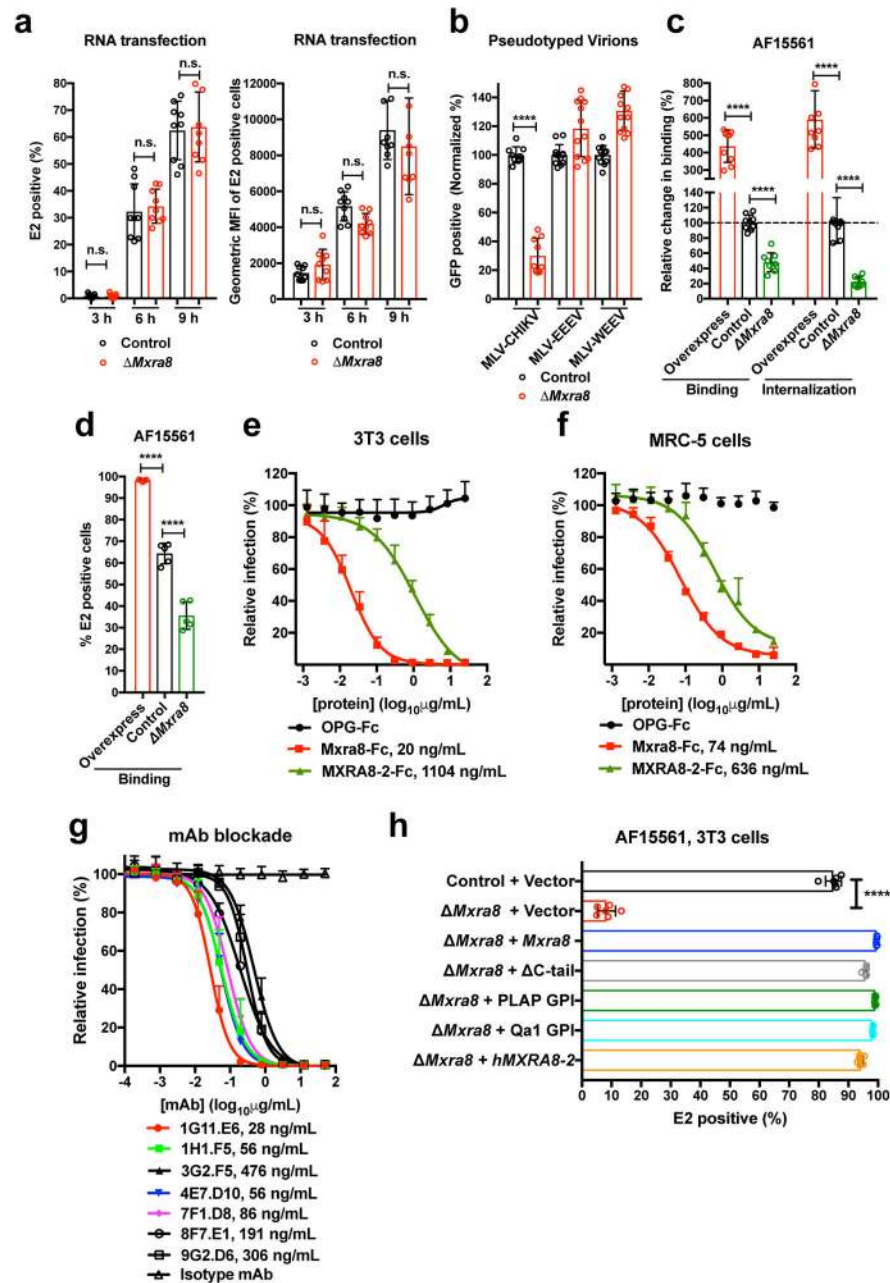


Figure 2. Mxra8 modulates CHIKV attachment and internalization

a. Transfection of CHIKV RNA into control or $\Delta Mxra8$ cells. Cells were analyzed for E2 expression (*left*, percent positive; *right*, mean fluorescence intensity; 3 experiments, $n = 9$; not significantly different (n.s.), two-tailed t-test with Holm-Sidak correction, mean \pm SD). **b.** MLV RNA encoding GFP and pseudotyped with alphavirus structural genes were added to control or $\Delta Mxra8$ cells. Data are from three (MLV-CHIKV, $n = 9$) or four (MLV-WEEV and MLV-EEEV, $n = 12$) experiments: (two-tailed t-test with Holm-Sidak correction, ***, $P < 0.0001$, mean \pm SD). **c-d.** CHIKV-AF15561 was incubated with control, $\Delta Mxra8$, and *Mxra8*-overexpressing MEFs at 4°C (**c**, *left* and **d**) or 37°C (**c**, *right*) as described in

Methods. Cells were harvested, and RNA (CHIKV and *Gapdh*) was measured by (c) RT-qPCR or surface E2 protein was analyzed by (d) flow cytometry (3 experiments, c, n = 9; d, n = 5; one-way ANOVA with Dunnett's test, ****, $P < 0.001$; mean \pm SD). e–f. Mxra8-Fc, MXRA8-2-Fc, or OPG-Fc were mixed with CHIKV-181/25 prior to infection of 3T3 (e) or MRC-5 (f) cells. Data are from two (MRC-5, n = 6) or three (3T3, n = 8–12) experiments: mean \pm SD. g. Blockade of CHIKV-181/25 infection in 3T3 cells with hamster anti-Mxra8 or isotype control mAbs (2 experiments, n = 6; mean \pm SD). h. Trans-complementation of Δ Mxra8 cells with vector, *Mxra8*, *Mxra8* Δ C-tail, *Mxra8* with GPI anchors (PLAP or Qa1-derived), or human *MXRA8-2* (3 experiments: (n = 6, one-way ANOVA with Dunnett's test, ****, $P < 0.001$, mean \pm SD).

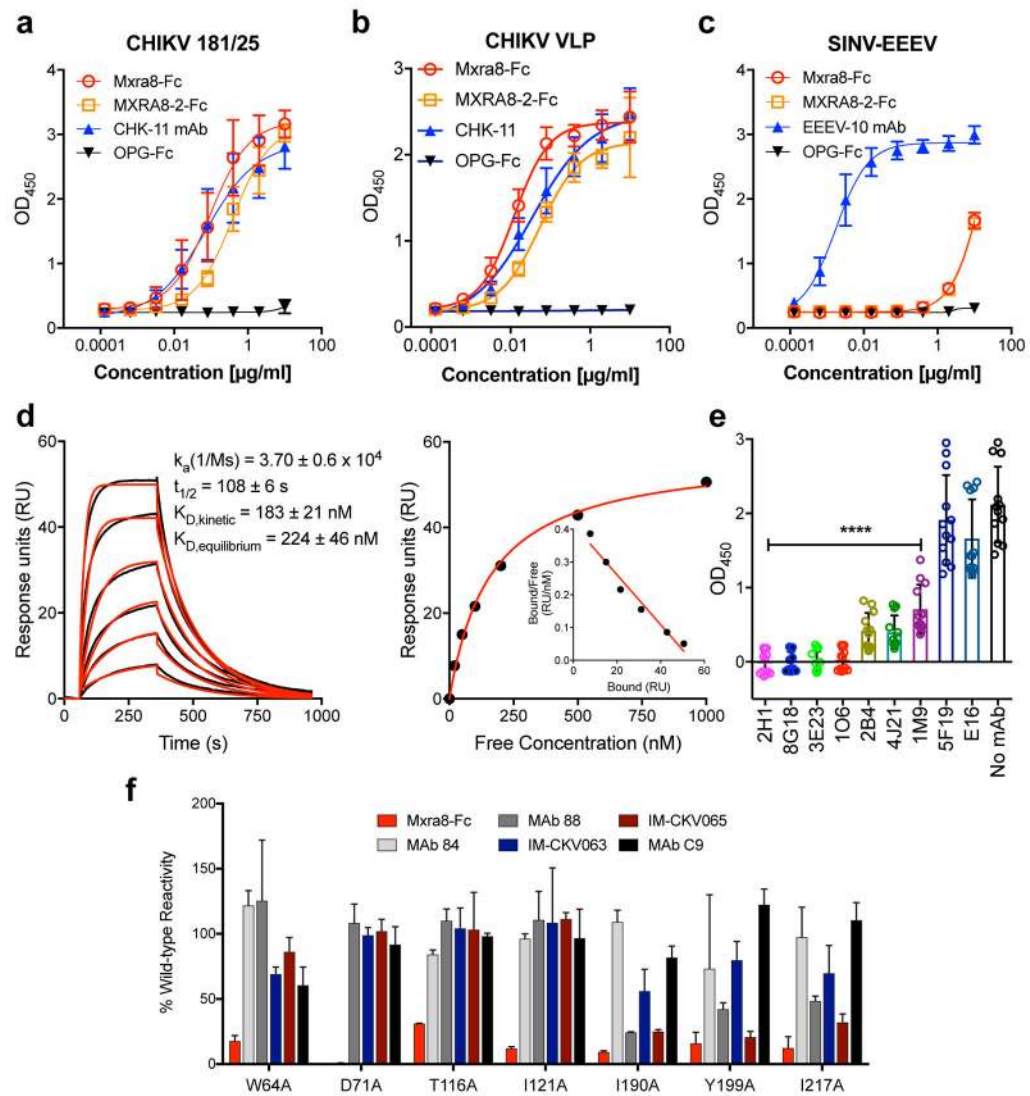


Figure 3. Direct binding of Mxra8 to CHIKV

a–c. Purified CHIKV-181/25 (**a**), CHIKV VLPs (**b**), or chimeric EEEV virions (**c**) were captured with anti-CHIKV or -EEEV human mAbs. Mxra8-Fc, MXRA8-2-Fc, or OPG-Fc and positive controls mAbs (CHK-11 or EEEV-10) were added. Data are from two (**b, c**) or three (**a**) experiments (**a**, $n = 8$; **b**, $n = 4$; **c**, $n = 6$): mean \pm SD. **d.** (*Left*) Sensograms of Mxra8 binding to CHIKV VLP. Experimental curves (black traces) were fit using a 1:1 binding model (red traces). (*Right*) Representative response curve for steady-state analysis, where binding is plotted versus Mxra8 concentration. *Inset.* Linear Scatchard plot (4 experiments; mean and standard error of the mean). **e.** Antibody blockade of Mxra8-Fc binding to CHIKV. Virus was incubated with indicated human mAbs against CHIKV, WNV (E16), or no mAb prior to the addition of Mxra8-Fc (4 experiments, $n = 12$; one-way ANOVA with Dunnett's test, ****, $P < 0.001$, mean \pm SD). **f.** Residues that result in loss of Mxra8-Fc binding to cell surface displayed CHIKV E2-E1. Residues are considered involved in the epitope if there is diminished binding without loss of protein integrity as judged by retention of interaction with mAbs (except for those previously mapped to a

specific residue). Graphs are shown for four A domain (W64, D71, T116, and I121A) and three B domain (I190, Y199, and I217) alanine mutations (see also Supplementary Table 3). Data are from two experiments.

Author Manuscript

Author Manuscript

Author Manuscript

Author Manuscript

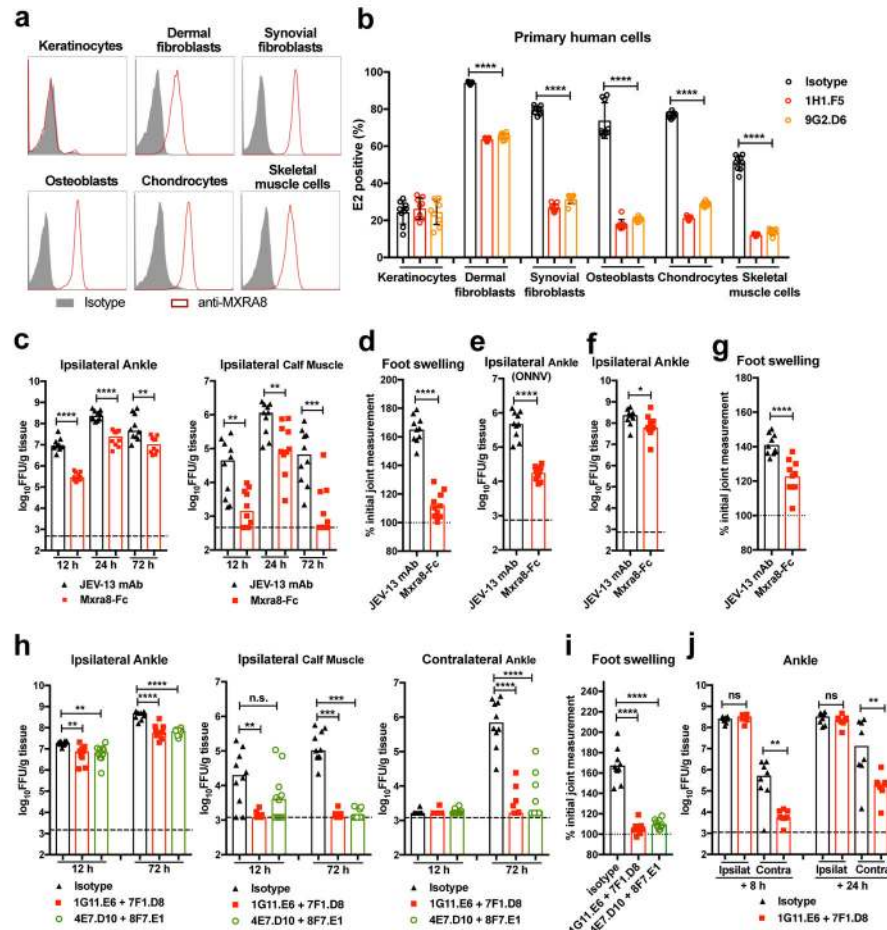


Figure 4. Mxra8 contributes to alphavirus pathogenesis

(a) Surface expression of MXRA8 on primary human keratinocytes, dermal fibroblasts, synovial fibroblasts, osteoblasts, chondrocytes, and skeletal muscle cells. One experiment of three is shown. (b) Cells were pre-incubated with anti-MXRA8 blocking mAbs prior to addition of CHIKV-AF15561 and processed for E2 staining (3 experiments, $n = 9$; one-way ANOVA with Dunnett's test, ****, $P < 0.0001$). c–d. Mxra8-Fc or JEV-13 mAb were incubated with CHIKV-AF15561 for 30 min prior to subcutaneous inoculation. (c) At 12, 24, and 72 h, CHIKV was measured in the ankle and calf muscle. (d) At 72 h, foot swelling was measured (2 experiments, $n = 10$; median viral titers: *, $P < 0.05$; **, $P < 0.01$; two-tailed Mann-Whitney test; mean foot swelling, ****, $P < 0.0001$; two-tailed unpaired t-test). e. Mxra8-Fc or JEV-13 mAb were mixed with ONNV immediately prior to subcutaneous inoculation. At 12 h, ONNV was measured in the ankle (2 experiments, $n = 10$; ****, $P < 0.0001$; two-tailed unpaired t-test; median values). f–g. Mxra8-Fc or JEV-13 mAb were administered via an intraperitoneal route 6 h prior to CHIKV-AF15561 inoculation in the footpad. At 24 h, CHIKV was measured in the ankle (f). At 72 h, foot swelling was measured (g) (2 experiments, $n = 10$; median viral titers: *, $P < 0.05$; two-tailed Mann-Whitney test; mean foot swelling, ****, $P < 0.0001$; two-tailed unpaired t-test). h–j. Pairs of anti-Mxra8 mAbs or isotype control hamster mAbs were administered via an intraperitoneal

route 12 h prior to (**h-i**) or 8 or 24 hours after (**j**) inoculation of CHIKV-AF15561. At 12 (**h**) and 72 (**h, j**) h, CHIKV was measured. At 72 h, foot swelling (**i**) was measured (2 experiments, (**h (left) and i**: n = 10; **, $P < 0.01$; ****, $P < 0.0001$; one-way ANOVA with Dunnett's test; **h (middle and right)**: n = 10; **, $P < 0.01$; ***, $P < 0.001$; ****, $P < 0.0001$; Kruskal-Wallis with Dunn's test; **j**: n = 8; **, $P < 0.01$; two-tailed Mann-Whitney test).